eLife

Reviewed Preprint
v2 • March 24, 2025
Revised by authors

Reviewed Preprint
v1 • November 5, 2024

Periosteal skeletal stem cells can migrate into the bone marrow and support hematopoiesis after injury

Tony Marchand, **Kemi E Akinnola**, **Shoichiro Takeishi**, **Maria Maryanovich**, **Sandra Pinho**, **Julien Saint-Vanne**, **Alexander Birbrair**, **Thierry Lamy**, **Karin Tarte**, **Paul S Frenette**, **Kira Gritsman**

Service d'hématologie Clinique, Centre Hospitalier Universitaire de Rennes, Rennes, France • UMR U1236, INSERM, Université Rennes, EFS Bretagne, Equipe Labellisée Ligue Contre le Cancer, Rennes, France • Ruth L. and David S. Gottesman Institute for Stem Cell and Regenerative Medicine, Albert Einstein College of Medicine, Michael F. Price Center, Bronx, United States • Department of Cell Biology, Albert Einstein College of Medicine, Michael F. Price Center, Bronx, United States • Department of Medical Oncology, Albert Einstein College of Medicine, Bronx, United States • Department of Pharmacology & Regenerative Medicine, University of Illinois at Chicago, Chicago, United States • Department of Dermatology, University of Wisconsin-Madison, Madison, United States • Laboratoire Suivi Immunologique des Thérapeutiques Innovantes, Centre Hospitalier Universitaire de Rennes, Rennes, France

eLife Assessment

The study presents **valuable** insights into the role of periosteal stem cells in bone marrow regeneration. The evidence is **convincing**. The data broadly support their claims and in line with state-of-art methodology. Future study on their model will help to strengthen their discovery further.

https://doi.org/10.7554/eLife.101714.2.sa3

Abstract

Summary

Skeletal stem cells have been isolated from various tissues, including periosteum and bone marrow, where they exhibit key functions in bone biology and hematopoiesis, respectively. The role of periosteal skeletal stem cells in bone regeneration and healing has been extensively studied, but their ability to contribute to the bone marrow stroma is still under debate. In the present study, we characterized a whole bone transplantation model that mimics the initial bone marrow necrosis and fatty infiltration seen after injury. Using this model and a lineage tracing approach, we observed the migration of periosteal skeletal stem cells into the bone marrow after transplantation. Once in the bone marrow, periosteal skeletal stem cells are phenotypically and functionally reprogrammed into bone marrow mesenchymal stem cells that express high levels of hematopoietic stem cell niche factors such as Cxcl12 and Kitl. In addition, using *ex vivo* and *in vivo* approaches, we found that periosteal skeletal stem cells are more resistant to acute stress than bone marrow mesenchymal stem cells. These results highlight the plasticity of periosteal skeletal stem cells and their potential role in bone marrow regeneration after bone marrow injury.

Introduction

Bone marrow mesenchymal stem cells (BM-MSCs) are rare self-renewing multipotent stromal cells which are capable of multilineage differentiation into osteoblasts, chondrocytes and adipocytes [1–3]. BM-MSCs are mostly localized around the blood vessels and represent an important component of the hematopoietic stem cell (HSC) microenvironment, also referred to as the niche. BM-MSCs closely interact with HSCs and secrete factors, including the C-X-C motif chemokine ligand (CXCL12) and stem cell factor (SCF), that control their self-renewal, differentiation, and proliferation capacities [4–9]. Several studies have used cell surface markers (CD51$^+$, PDGFRα$^+$, Sca-1$^+$) or reporter mice (*Lepr*-cre, Nestin (*Nes*)-GFP, *Ng2*-cre) to describe distinct BM-MSC populations with significant overlap [4–6,10–13].

Recent studies have suggested that the periosteum, a thin layer of fibrous material that covers the surface of long bones, is a source of skeletal stem cells (SSCs) for bone regeneration [14–18]. These periosteum SSCs (P-SSCs) have been described as sharing some characteristics with BM-MSCs [14–16]. However, the relationship between these different stromal cell populations is poorly understood and the distinction between MSCs and SSCs remains controversial.

While the bone marrow is classically known as a major source of MSCs, the bone cortex represents a richer source of colony-forming units-fibroblasts (CFU-F) [12,19,20]. It has been suggested that bone regeneration is mediated by both endochondral and intramembranous ossification and that the periosteum plays an important role in bone regeneration after injury [15,16,21–23]. However, there is little information on the function of P-SSCs, aside from their crucial role in bone healing and remodeling, and whether they contribute to bone marrow regeneration.

In the present study, we developed and characterized a whole bone transplantation model to study bone marrow regeneration, in which an intact adult femur is transplanted subcutaneously into a recipient mouse [24]. Shortly after transplantation, bone marrow architecture in the transplanted femur, hereafter referred to as the graft, is severely altered with an expansion of adipocytes that mimics the fatty infiltration classically observed in the bone marrow after chemotherapy or radiation [25]. This initial destruction of the bone marrow microenvironment is followed by a progressive regeneration of blood vessels and the BM-MSCs network. The graft is progressively colonized by host-derived HSCs, allowing hematopoiesis to resume. Unexpectedly, we found that P-SSCs can migrate into the bone marrow and acquire BM-MSC niche functions, making them capable of supporting hematopoiesis through the *in vivo* expression of specific niche genes, such as *Cxcl12* and *Kitl*. In addition, we found that BM-MSCs and P-SSCs display different metabolic profiles, and that P-SSCs exhibit higher resistance to transplantation-induced stress. In conclusion, our study demonstrates the high plasticity of P-SSCs and highlights their potential contribution to bone marrow stroma regeneration after injury.

Results

The whole bone transplant model recapitulates physiological regeneration of the bone marrow

In order to study the mechanisms involved in bone marrow regeneration, we employed a model system based on the subcutaneous transplantation of an intact adult femur into non-conditioned age and sex-matched recipient mice (**Figure 1A**). The bone transplantation is followed by a rapid and massive depletion of bone marrow cells in the engrafted femur with a cell viability reaching below 10% at 24 hours after transplantation (Figure S1A). Notably, bone marrow necrosis

following bone transplantation is associated with the replacement of hematopoietic cells in the graft femur by marrow adipocytes, similar to the effects of chemotherapy or irradiation [25,26] (Figure S1B). Following bone transplantation, we observed a progressive increase in bone marrow cellularity over time with no significant difference in cellularity between the graft and host femurs at five months following transplantation (**Figure 1B**). Regeneration of the bone marrow compartment is associated with a reduction in adipogenic infiltration, as revealed by staining with the anti-perilipin antibody at 4 months post-transplantation (Figure S1B). Additionally, the absolute number of graft BM-MSCs, defined as $CD45^{-}Ter119^{-}CD31^{-}CD51^{+}CD140\alpha^{+}$ cells by flow cytometry[12], also increased over time, with no difference between the graft and host femurs at five months following transplantation (**Figure 1B**). We also observed a progressive increase in the number of $Lin^{-}Sca1^{+}cKit^{+}CD48^{-}CD150^{+}$ phenotypic HSCs in the graft femur over time (**Figure 1B**). Although the absolute HSC numbers in the graft did not reach HSC numbers as detected in the host femur after five months (**Figure 1B**), no differences were observed in the numbers of hematopoietic progenitors or in the frequencies of hematopoietic cell populations between the host and graft femurs (Figure S1C and S1D). These data suggests that bone transplantation causes significant bone marrow injury, followed by a recovery process.

Hematopoiesis is a highly regulated and essential process by which all the differentiated blood cells are produced. To investigate whether functional hematopoietic progenitors fully recover in graft femurs, we performed a non-competitive bone marrow transplantation assay, in which we transplanted either graft or host bone marrow cells into lethally irradiated recipients at five months after bone transplantation (**Figures 1C** and S2A). The survival of lethally irradiated recipients remained equal in both groups, with 100% of recipients surviving throughout the length of the experiment. Chimerism analysis revealed robust engraftment of recipient mice with hematopoietic cells derived from the engrafted femurs, indicating that HSCs and progenitors derived from graft femurs can sustain long-term hematopoiesis upon transplantation (**Figure 1D**). We also observed no significant differences in donor cell contribution to myeloid or lymphoid lineages between the two groups (**Figure 1E**). Altogether, these data establish our bone transplantation model as a useful tool to study bone marrow and HSC niche regeneration.

Graft BM-MSCs are graft-derived and progressively express HSC niche factors during regeneration

Next, we aimed to determine the origin of the hematopoietic and stromal cell populations in the graft bone marrow. To achieve this, we took advantage of the $Rosa^{mT/mG}$ and ubiquitin C (UBC) promoter driven-GFP mouse models, in which all cells are labeled by red and green reporters respectively [27,28]. We transplanted femurs isolated from UBC-GFP mice into $Rosa^{mT/mG}$ recipients and quantified endothelial cells, BM-MSCs, and hematopoietic cells in the graft (**Figures 2A** and **2B**). Corroborating the results of Picoli et al., we observed that at five months post transplantation, over 98% of the graft BM-MSCs originated from the graft femur, while over 99% of the hematopoietic cells in the graft originated from the host mouse[24] (**Figures 2C** and **2D**). Interestingly, endothelial cells were derived from both the host and the graft, suggesting the contribution of different progenitors. To further assess endothelial regeneration within the context of bone transplantation, we conducted a transplantation experiment in which femurs from Cdh5 (VE-cadherin)-CreER; iTdTomato[29] mice were transplanted into WT recipients. Confocal analysis was performed fifteen days (Figure S3A) and one month (Figure S3B) after transplantation. This revealed the presence of VE-cadherin-labeled vessels within the periosteum and crossing the cortical bone of the graft. This result demonstrates that endothelial regeneration occurs at an early stage following bone transplantation. Furthermore, when femurs from UBC-GFP mice were transplanted into Cdh5-CreER;iTdTomato mice, contributions of both recipient VE-cadherin-labelled vessels and UBC-GFP vessels were observed five months later. This result once again demonstrated the dual contribution of endothelial cells to the grafted femur (Figure S3C).

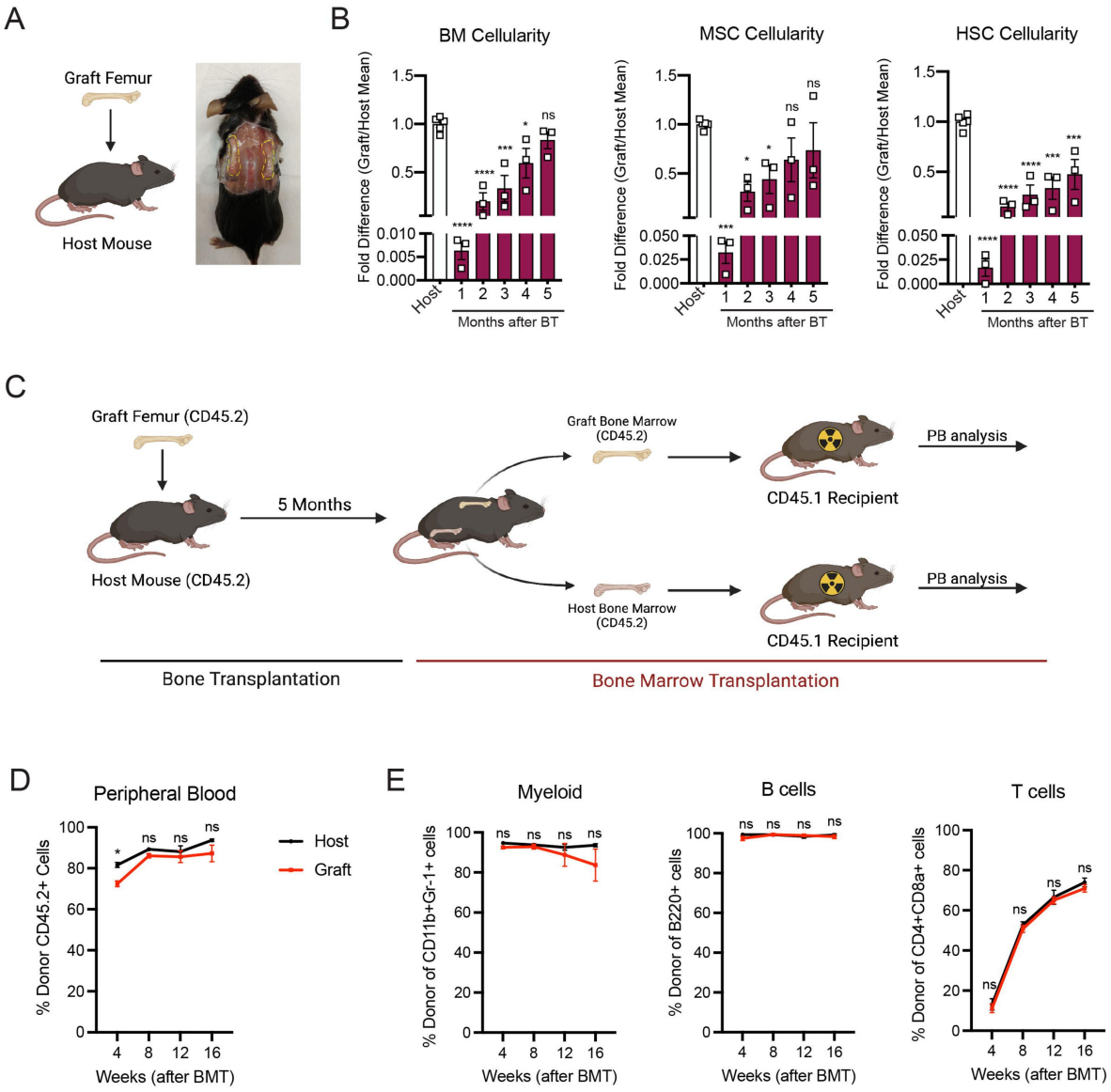

Figure 1.

Whole bone transplantation is a good model to study bone marrow regeneration.

A. Schematic and picture of the bone transplantation procedure.
B. Fold difference quantification of graft femur/host femur cellularity normalized to mean host femur cellularity. Total graft bone marrow cells, BM-MSCs and HSCs were analyzed monthly until 5 months after bone transplantation (BT) (n=3). Ordinary one-way ANOVA with Dunnett multiple comparisons was used to determine statistical significance.
C. Schematic illustration of the non-competitive repopulating assay after bone transplantation.
D. Donor HSC contribution of graft and host recipients at 4 weeks after bone marrow transplantation (n=10).
E. Quantification of tri-lineage (myeloid, B lymphoid, and T lymphoid cells) engraftment 4 weeks post transplantation (n=10).
This figure was created using *BioRender.com*.

Furthermore, we did not detect any cells derived from the graft in the host femurs (data not shown). These results are consistent with data obtained from ossicle-based experiments, where MSC-seeded ossicles are colonized by recipient-derived hematopoietic cells [10,30–33].

BM-MSCs are a major constituent of the hematopoietic niche, secreting maintenance factors that support HSCs and hematopoietic progenitors[4–6,11,34,35]. To test for HSC niche supportive activity of graft BM-MSCs, we utilized *Nes*-GFP reporter mice to isolate BM-MSCs after bone transplantation. Previous work from our group has shown that *Nes*-GFP marks mouse MSCs with HSC-niche function within the bone marrow[10]. Since our previous analysis (**Figure 2D**) revealed that all of the graft BM-MSCs originate from the graft itself, we transplanted *Nes*-GFP femurs into *Nes*-GFP recipient mice and sorted CD45$^-$Ter119$^-$CD31$^-$*Nes*-GFP$^+$ BM-MSCs from donor and recipient mice for analysis at different time points (**Figure 2E**). Since we did not detect circulation of BM-MSCs between host and graft bone marrow in our bone transplantation experiments (data not shown), this strategy allowed us to compare host and graft BM-MSCs using equivalent markers. In addition to the previously described increase over time in the absolute number of BM-MSCs in the graft femur (**Figure 1B**), we observed a progressive increase in the expression of the HSC-niche genes *Cxcl12* and *Kitl* (which encodes Scf), reaching a plateau at five months post-transplantation (**Figure 2F**). Similarly, no differences were observed between host and graft femurs in the expression levels of additional niche factors, including *osteopontin* (*Opn*)[36,37], *angiopoietin-1* (*Angpt1*)[38], and *vascular cell adhesion molecule-1* (*Vcam1*)[39,40] at five months (Figure S2B). In this experiment, host and graft BM-MSCs also had similar CFU-F activity at five months (Figure S2C). Altogether, these results show that by five months post-bone transplantation, the niche-supportive and *ex vivo* clonogenic functions of graft BM-MSCs are restored and are similar to the activity of native host BM-MSCs.

P-SSCs but not BM-MSCs expand early after bone transplantation

SSCs are multipotent cells of the skeletal lineage that are important for bone development, repair, and homeostasis[41,42]. SSCs have been identified in the periosteum (P-SSCs), compact bone, and bone marrow[10,11,15,43]. Similar to BM-MSCs, P-SSCs have been shown to have CFU-F activity and the ability to differentiate into osteoblasts, chondrocytes, and adipocytes[14,16,44]. Due to the severe necrosis and depletion of the marrow cavity content that we observed following bone transplantation (**Figures 1B** and S1A), we hypothesized that cells derived from the compact bone and/or the periosteum could potentially contribute to stromal marrow regeneration. We first analyzed the cellularity of graft bone marrow, compact bone, and periosteum at different early time points following transplantation. While the number of live cells within the bone marrow and compact bone were drastically reduced in the first 24 hours post transplantation, we unexpectedly observed a significant but transient increase in live periosteal cells (**Figures 3A** and S4A). Moreover, while most of the bone marrow cells were depleted shortly after transplantation (Figures S1A and S4A), cell viability was not affected in the periosteum within this time frame (**Figures 3A** and S4B). To quantify P-SSCs and BM-MSCs by flow cytometry, we used the combination of CD51 and CD200, as these markers have been well-validated in both tissues[14,16,45]. Within the CD45$^-$Ter119$^-$ CD31$^-$ fraction of live periosteal cells, we confirmed that CD51$^+$CD200$^+$ P-SSCs had the highest CFU-F activity and were also capable of trilineage differentiation (Figures S4C-S4E). Flow cytometric analysis confirmed an expansion of P-SSCs starting at day 3 post transplantation and peaking at day 8 (**Figure 3B** and S4F). These results were confirmed by confocal microscopy analysis of *Nes*-GFP graft femurs transplanted into WT mice and stained for Periostin, a matricellular protein highly expressed by periosteal cells[15,46–49]. We detected an expansion of *Nes*-GFP$^+$ skeletal progenitors[50] within the periosteum with a peak at day 8 (**Figure 3C**), similar to the expansion kinetics that we detected by flow cytometry. Interestingly, by day 15, we could detect Nes-GFP$^+$ cells outside of the periosteum layer stained by an anti-periostin antibody and in the compact bone (**Figure 3C**).

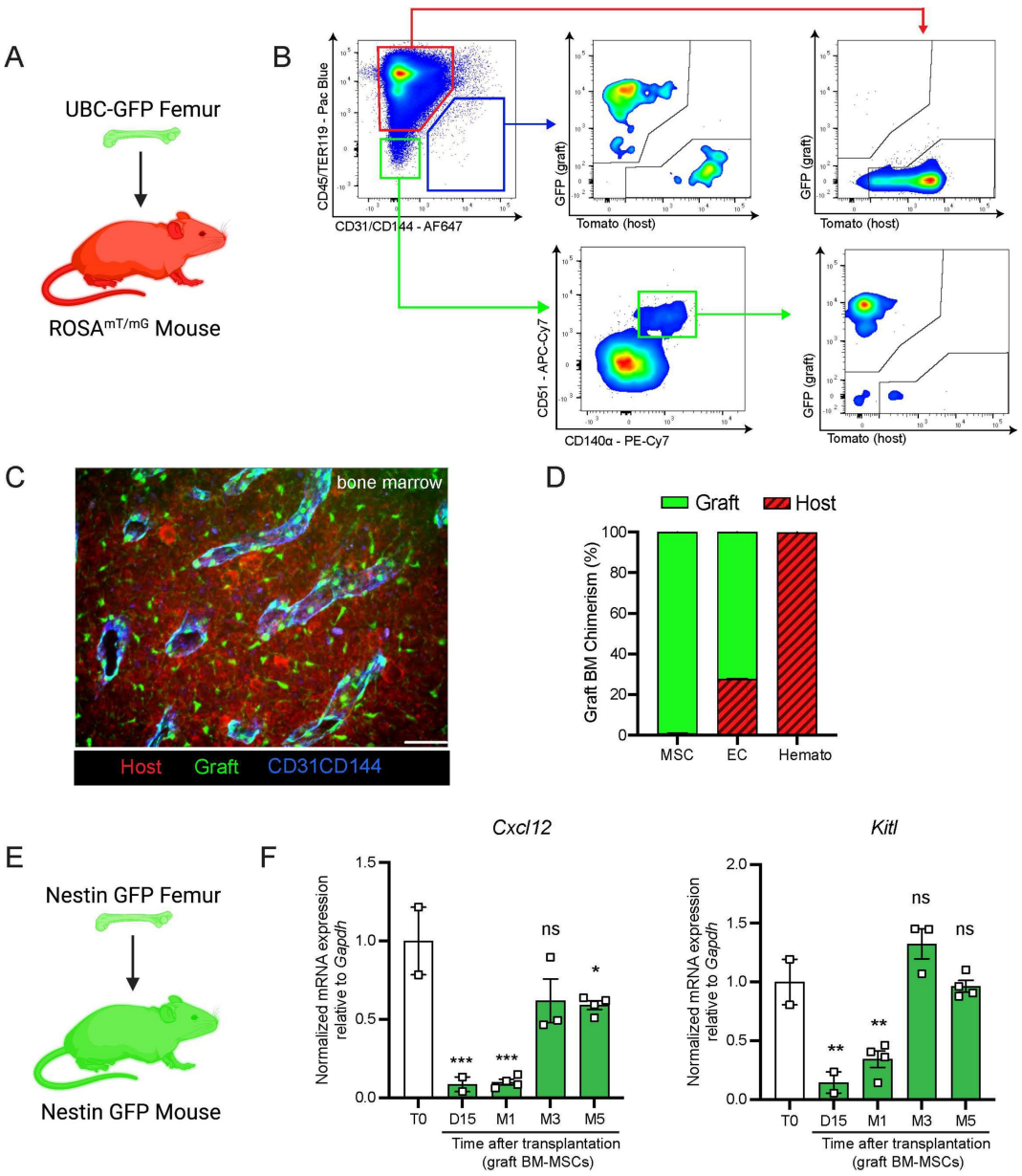

Figure 2.

Regenerating BM-MSCs are graft-derived and express HSC niche factors.

A. Schematic of a UBC-GFP femur transplanted into a Rosa$^{mT/mG}$ mouse.
B. Representative FACS plots showing the gating strategy to determine the origin of the different cell fractions in the graft 5 months after transplantation of a UBC-GFP femur into a Rosa$^{mT/mG}$ mouse.
C. Representative whole-mount confocal z-stack projections of a UBC-GFP bone transplanted into a Rosa$^{mT/mG}$ recipient 5 months after transplantation. Vascularization was stained with anti-CD31 and anti-CD144 antibodies. Scale bar = 100µm (n=2 mice).
D. Origin of graft BM-MSCs, endothelial cells (EC) and hematopoietic cells (Hemato) analyzed by flow cytometry 5 months after bone transplantation (n=2).
E. Schematic of the *Nes*-GFP femur transplantation into a *Nes*-GFP mouse recipient.
F. Quantitative RT-PCR analysis of mRNA expression of *Cxcl12* and *Kitl* expression relative to *Gapdh* in graft *Nes*-GFP^{+} BM-MSCs compared to steady-state *Nes*-GFP^{+} BM-MSCs at multiple time points after transplantation (n= 2-4 mice per time point). One-way ANOVA with Dunnett multiple comparisons was used to determine statistical significance.
Data are represented as the mean ± SEM. Unless otherwise noted, statistical significance was determined using unpaired two-tailed Student's t test. *p<0.05. ** p<0.01. *** p<0.001. ****p<0.0001. This figure was created using *BioRender.com*.

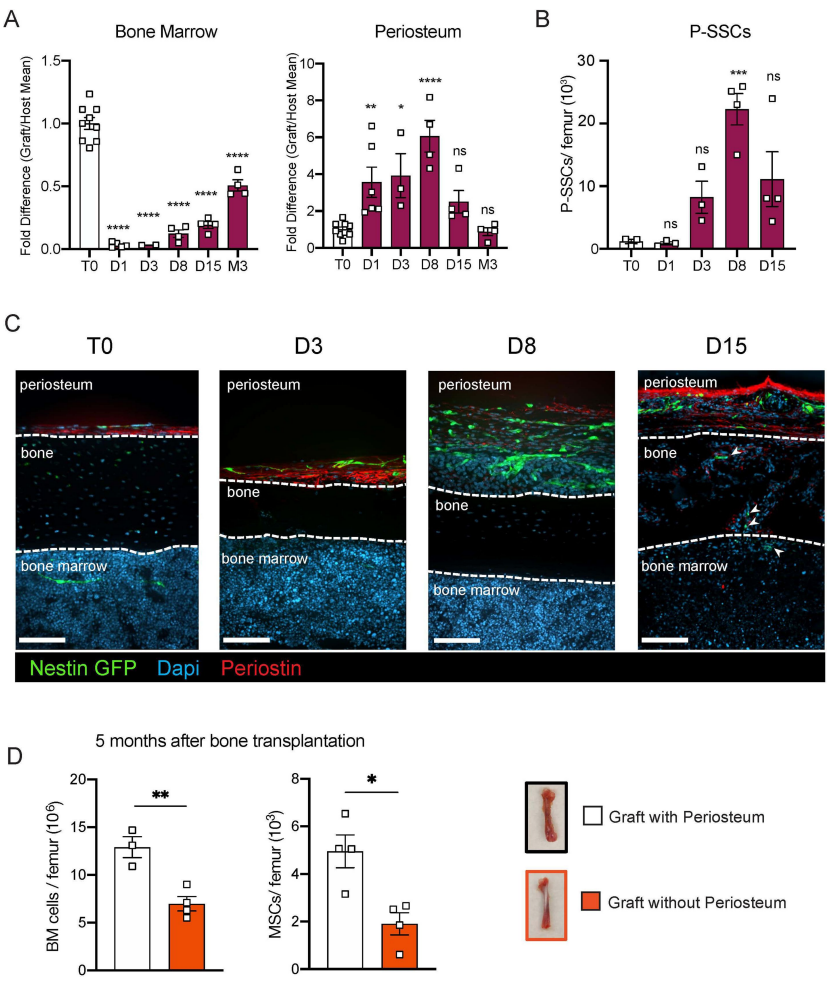

Figure 3.

P-SSCs remain viable and expand after bone transplantation, in contrast to BM-MSCs.

A. Flow cytometric quantification of fold difference of total graft bone marrow and periosteum cellularity to total steady state cellularity. Different time points early after transplantation were analyzed (n=2-8). One-way ANOVA with Dunnett multiple comparisons was used to determine statistical significance.
B. Absolute number of $CD45^{-}Ter119^{-}CD31^{-}CD51^{+}CD200^{+}$ P-SSCs at steady state and 1-, 8- and 15-days post transplantation (n=3-4 mice per time point). One-way ANOVA with Dunnett multiple comparisons was used to determine statistical significance.
C. Representative whole-mount confocal z-stack projections of *Nes*-GFP^{+} bone graft at steady state, three-, eight-, and fifteen-days post transplantation. Three independent experiments yielded similar results. Arrowheads point at *Nes*-GFP^{+} cells within the bone and bone marrow. Scale bar = 100µm
D. Total bone marrow cellularity and BM-MSC absolute number 5 months after transplantation of bones with or without intact periosteum (n=3-4 mice per group).
Data are represented as the mean ± SEM. Unless otherwise noted, statistical significance was determined using unpaired two-tailed Student's t test. *p<0.05. ** p<0.01. *** p<0.001. ****p<0.0001.

To evaluate the potential role of the periosteum in overall bone marrow regeneration, we compared the regenerative capacity of transplanted femurs with intact periosteum to that of femurs in which the periosteum was mechanically removed (**Figure 3D**). At five months after transplantation, total cellularity and BM-MSC number were significantly reduced in femurs lacking the periosteum, highlighting a potentially critical role for the periosteum and P-SSCs during bone marrow regeneration.

P-SSCs are more resistant to stress than BM-MSCs

Due to the ability of P-SSCs to survive bone transplantation, as opposed to BM-MSCs, we explored the intrinsic differences between BM-MSCs and P-SSCs. Using RNA sequencing, we analyzed the transcriptional differences between $CD51^+CD200^+$ P-SSCs and BM-MSCs at steady-state. Gene set enrichment analysis (GSEA) revealed that P-SSCs were positively enriched for gene sets associated with stemness and negatively enriched for gene sets associated with proliferation (**Figure 4A**). These results are in line with qPCR analysis showing that P-SSCs express high levels of the cell cycle inhibitor genes *Cdkn1a* and *Cdkn1c,* and low levels of the cell cycle progression gene *Cdk4* at steady state (**Figures 4B**). Additionally, flow cytometric analysis revealed that, compared to BM-MSCs, P-SSCs are less metabolically active, as shown by decreased glucose uptake as assessed by 2-(N-(7-Nitrobenz-2-oxa-1,3-diazol-4-yl)Amino)-2-Deoxyglucose (2-NDBG) (**Figure 4C**). This led us to hypothesize that P-SSCs are more resistant to stress than BM-MSCs.

These observations led us to also use RNA sequencing to compare steady-state P-SSCs to P-SSCs at three days after bone transplantation. We chose the 72-hour time point to capture the time when P-SSCs are expanding but have not yet hit the peak of expansion at around day eight. We found that while steady-state P-SSCs and day three graft P-SSCs are quite distinct from steady-state BM-MSCs, there is a clear variance starting to occur between the two P-SSC populations (Figure S5A). As early as three days post bone transplantation, we observed a downregulation of extracellular matrix (ECM) factors such as fibromodulin (*Fmod*) and nidogen 1 (*Nid1*) in the graft P-SCCs (Figure S5B). Additionally, gene set enrichment analysis (GSEA) comparing steady-state P-SSCs with graft P-SSCs, revealed an upregulation of cell cycle and DNA replication signatures and downregulation of ECM-receptor interaction and glutathione metabolism (Figure S5C), indicating that a change in the P-SSCs phenotype occurs early after bone transplantation.

Low levels of reactive oxygen species (ROS) and high expression of antioxidant enzymes are mechanisms that help stem cells to avoid stress-induced cell death [51,52]. Thus, we measured ROS levels by staining cells with the superoxide indicator dihydroethidium (DHE). At steady state, flow cytometric analysis revealed that P-SSCs had lower levels of cellular ROS than BM-MSCs (**Figure 4D**). Under physiological conditions, cells can maintain low ROS levels by expressing antioxidant enzymes. Indeed, qPCR analysis revealed higher expression of three major ROS-detoxifying enzymes genes: superoxide dismutase (*Sod1*), glutaminase (*Gls*) and glutathione peroxidase (*Gpx1*), in sorted $CD51^+CD200^+$ P-SSCs than in $CD51^+CD200^+$ BM-MSCs (**Figure 4E**). Altogether, these results suggest that P-SSCs are more stress-resistant than BM-MSCs, which may leave P-SSCs poised to proliferate in response to transplantation.

The location of the periosteum on the exterior of the bone, exposing P-SSCs to a higher oxygen tension than BM MSCs, may be a contributing factor to the observed differences in resilience between P-SSCs and BM-MSCs. Therefore, to determine whether the anatomic location of BM-MSCs and P-SSCs is the primary determinant of their differential stress response, we performed an *ex vivo* culture experiment designed to subject BM-MSCs and P-SSCs to equivalent levels of stress while in the same environment. After short-term *ex vivo* expansion of total bone marrow and periosteal cells, we performed a lineage depletion of $CD45^+$ hematopoietic cells in both fractions. Purified P-SSCs and BM-MSCs were then maintained for 12 hours in serum-free culture media to stress the cells and mimic the nutrient deprivation that occurs immediately following bone transplantation (**Figure 4F**). Flow cytometric analysis of activated caspase-3/7 revealed that after 12 hours in serum-free media, BM-MSCs exhibited a significantly higher level of apoptosis

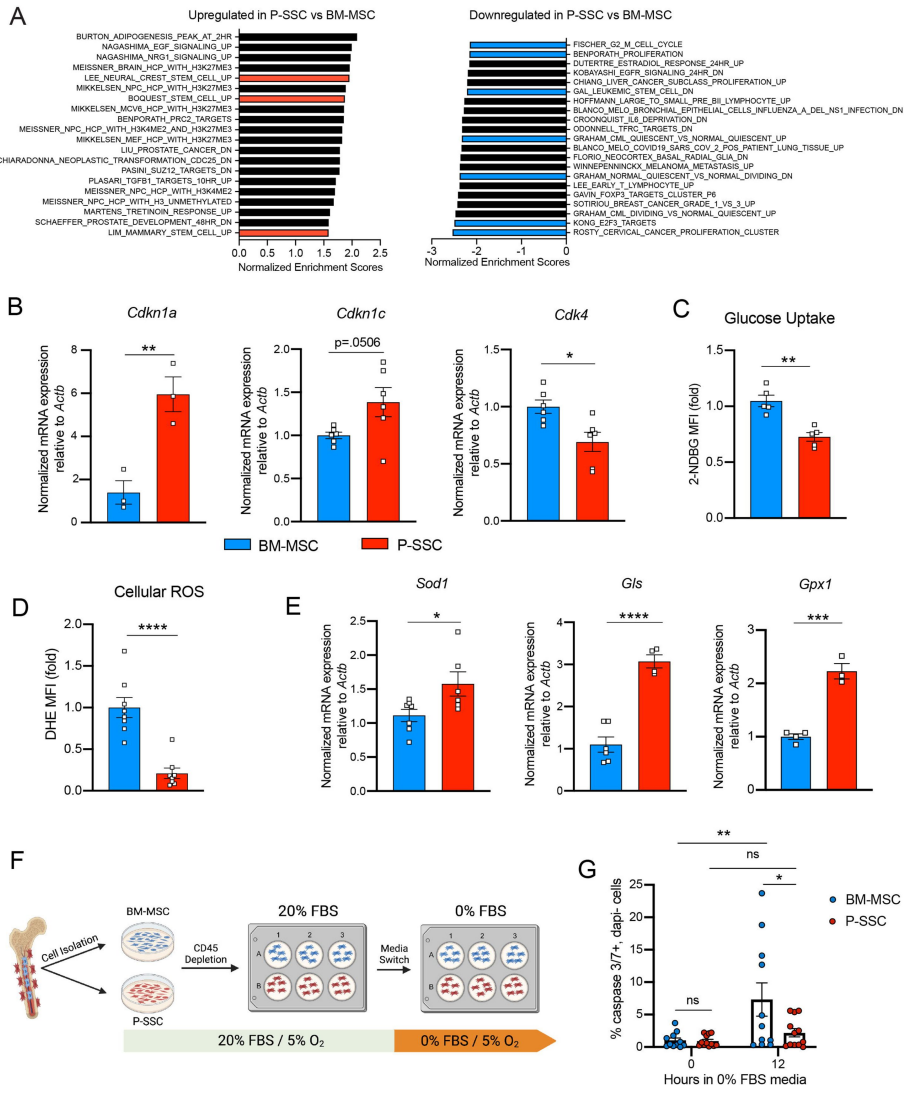

Figure 4.

Periosteal SSCs have a metabolic profile conferring a resistance to stress

A. Gene set enrichment analysis (GSEA) plots comparing P-SSCs versus BM-MSCs at steady state (n=3 per group).
B. Quantitative RT-PCR analysis of mRNA expression of *Cdkn1a*, *Cdkn1c*, *Cdk4* relative to *Actb* in sorted CD45$^-$Ter119$^-$CD31$^-$CD51$^+$CD200$^+$ BM-MSCs and P-SSCs (n=3-6 per group).
C. Flow cytometric analysis of glucose uptake at steady state in CD45$^-$Ter119$^-$CD31$^-$CD51$^+$CD200$^+$ BM-MSCs and P-SSCs (n=5 per group).
D. Quantification of cellular ROS at steady state in CD45$^-$Ter119$^-$CD31$^-$CD51$^+$CD200$^+$ BM-MSCs and P-SSCs (n=8 per group).
E. Quantitative RT-PCR analysis of mRNA expression of *Sod1*, *Gls* and *Gpx1* relative to *Actb* in sorted CD45$^-$Ter119$^-$CD31$^-$CD51$^+$CD200$^+$ BM-MSCs and P-SSCs (n=3-7 per group).
F. Schematic illustration of the protocol for the *in vitro* apoptosis assay. BM-MSCs and P-SSCs were isolated and digested before plating in a 10cm dish. At near confluence, cells underwent CD45 lineage depletion and plated into multi-well plates. At near confluence, medium was switched from 20% FBS to 0% FBS. Cells were analyzed at the time of medium switch and 12 hours.
G. Percentage of apoptotic BM-MSCs and P-SSCs cultured under 5% O_2 at baseline and 12 hours after being in 0% FBS serum conditions (n=11-12 per group). Two-way ANOVA with Tukey's multiple comparisons test was used to determine statistical significance.
Data are represented as the mean ± SEM. Unless otherwise noted, statistical significance was determined using unpaired two-tailed Student's t test. *p<0.05. ** p<0.01. *** p<0.001. ****p<0.0001. This figure was created using *BioRender.com*.

compared to P-SSCs (**Figures 4G** and S5D). These results suggest that P-SSCs are more intrinsically resilient than BM-MSCs, even when they are subjected to similar stress conditions in an equivalent environment.

P-SSCs as a source of functional BM-MSCs during regeneration

As we observed that bone transplantation was followed by a depletion of bone marrow cellularity with an early expansion of P-SSCs, and that transplantation of bones without periosteum negatively impacts graft regeneration (**Figures 3D**), we hypothesized that proliferating P-SSCs migrate into the bone marrow and contribute to stromal regeneration. To test this hypothesis, we removed the periosteum from WT femurs and wrapped these femurs with the periosteum isolated from UBC-GFP mice (**Figure 5A** and **5B**). We then transplanted these bones into WT host mice and observed GFP$^+$ cells within the compact bone at five months after transplantation (**Figure 5C**), consistent with the well-described role of the periosteum in bone remodeling [15,16,53]. Consistent with our hypothesis, we also observed GFP$^+$ cells enwrapping endomucin-stained sinusoids and forming a network, similar to the perivascular nature of BM-MSCs[9,10]. (**Figure 5C**).

Flow cytometric analysis of the graft at five months post-transplantation confirmed the presence of periosteum-derived GFP$^+$ MSCs within the bone marrow cavity (Figure S6A). Importantly, while P-SSCs do not express *Cxcl12* or *Kitl* at steady state, periosteum-derived GFP+ BM-MSCs expressed these niche cytokines at a similar level to control sorted *Nes*-GFP+ BM-MSCs (**Figure 5D**). We also quantified the expression of the niche factors *Angpt1* and *Opn.* Similarly, we found that *Angpt1* expression in the graft GFP$^+$ BM-MSCs reached the level of control BM-MSCs, while *Opn* expression was higher in GFP$^+$ BM-MSCs than in control *Nes*-GFP+ BM-MSCs at five months after transplantation (Figure S6B). However, *Opn* has been shown to be upregulated in settings of inflammation, injury and migration[54–56]. Therefore, the moderate increase in *Opn* expression level in graft BM-MSCs compared to steady state BM-MSCs could be due to a residual inflammatory effect of bone transplantation. These results show that P-SSCs can both migrate into the bone marrow cavity and upregulate HSC maintenance genes to support hematopoiesis.

To confirm these results, we took advantage of a previously described transgenic mouse model in which an inducible Cre is placed under the promoter of the *Periostin* gene (*Postn*^{MCM}), hereafter referred to as *Postn*-cre^{ER} [57]. *Postn* encodes the secreted matricellular protein Periostin, and is highly expressed by periosteal cells and upregulated during bone healing and formation[15]. While *Postn* is expressed by multiple cell types, including but not limited to osteoblasts and fibroblasts[47,49,58], its high expression in P-SSCs compared with BM-MSCs (Figure S7A) makes it a useful marker to distinguish endogenous BM-MSCs from periosteum-derived BM-MSCs after bone transplantation. We crossed the *Postn*-cre^{ER} line with ROSA26-loxP-stop-loxP-tdTomato reporter (Tomato) mice to be able to lineage trace P-SSCs. We transplanted femurs from *Postn*-cre^{ER};tdTomato mice into WT CD45.2 recipient mice, and then injected the host mice with tamoxifen shortly after transplantation to induce Cre recombination and Tomato expression in periosteal cells (**Figure 6A**). At early time points following bone transplantation, we see Tomato$^+$ cells confined to the periosteum and located perivascularly. At 21 days after transplantation, we observe Tomato+ cells migrating into the bone marrow (**Figure 6B**). By five months after transplantation, we observe robust Tomato$^+$ labeling in the bone marrow located around the vasculature by confocal imaging (Figure S7B), consistent with our prior observations (**Figure 5C**). Additionally, flow cytometric analysis revealed that an average of 85.4% (range: 65.0% – 94.5%) of the BM-MSCs within the engrafted bone marrow were Tomato$^+$, indicating a periosteal origin (**Figures 6C** and S7C).

We then wanted to assess our *Postn* mouse model using irradiation as a more physiologically relevant model of bone marrow injury, and to compare the effects of localized irradiation to femur transplantation on P-SSC plasticity. Single hindlimbs of *Postn*-cre^{ER};tdTomato mice were irradiated in order to compare the effects of irradiation within the same mouse (Figure S7D). While a clear

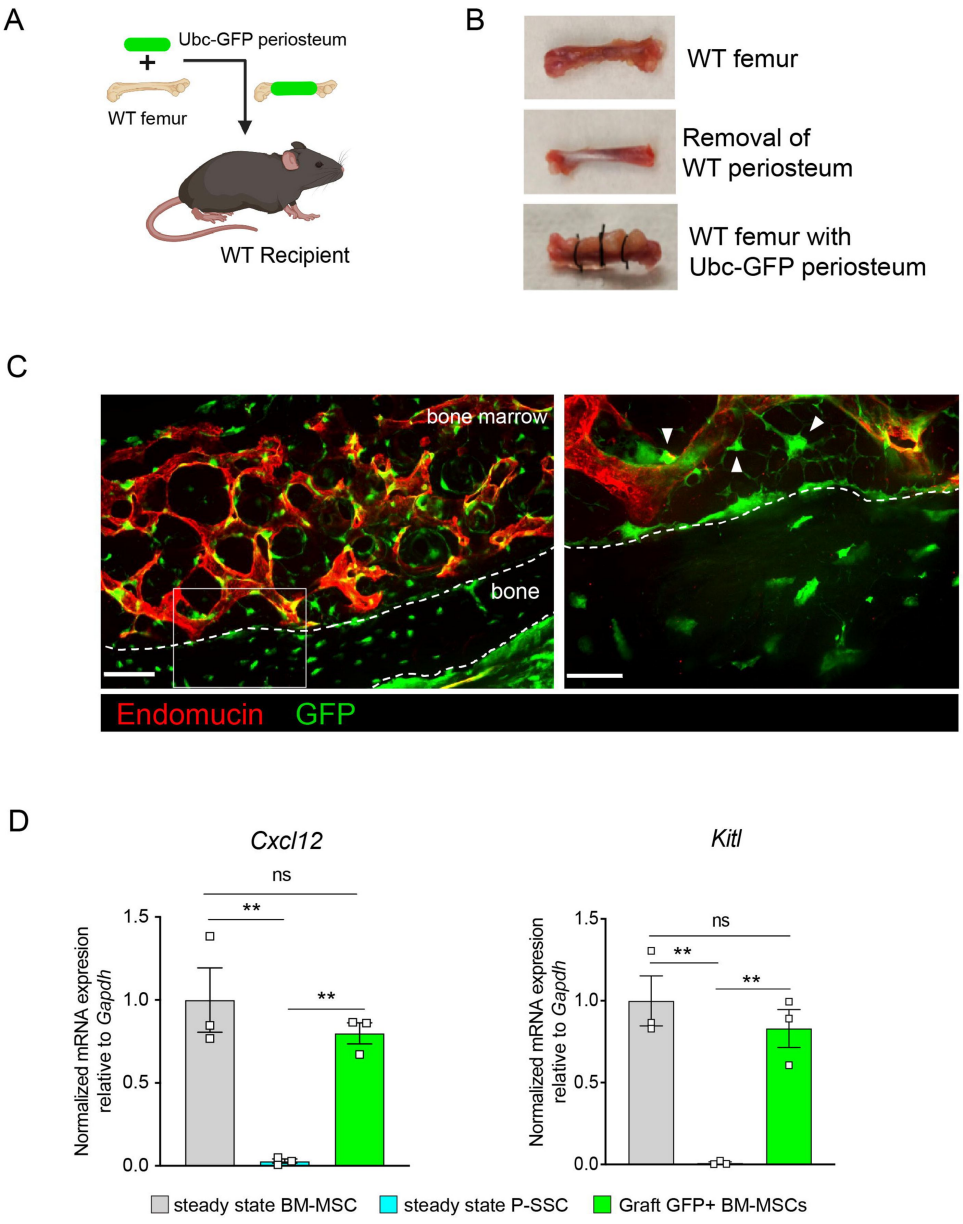

Figure 5.

Periosteal SSCs migrate into the bone marrow and support stromal regeneration after bone transplantation.

A. Schematic of the transplantation of a WT bone enwrapped with periosteum from a UBC-GFP mouse donor into a WT recipient mouse.

B. Pictures illustrating the transplantation of a WT bone enwrapped with periosteum from a UBC-GFP mouse donor into a WT recipient mouse.

C. Representative whole-mount confocal z-stack projections of wild-type bone graft enwrapped with periosteum from a UBC-GFP mouse donor into a WT recipient mouse 5 months after transplantation. Three independent experiments yielded similar results. Right panel: arrows pointing to GFP^+ periosteum located perivascularly. Scale bar = 50µm (left panel) and 20µm (right panel)

D. Quantification of *Cxcl12* and *Kitl* mRNA levels relative to *Gapdh* in sorted control $CD45^-Ter119^-CD31^-Nestin\text{-}GFP^+$ BM-MSCs, $CD45^-Ter119^-CD31^-CD51^+CD200^+$ P-SSCs, and $CD45^-Ter119^-CD31^-CD51^+CD200^+GFP^+$ periosteum-derived graft BM-MSCs (n = 3-4 per group). One-way ANOVA with Tukey's multiple comparisons was used to determine statistical significance.

Data are represented as the mean ± SEM. Unless otherwise noted, statistical significance was determined using unpaired two-tailed Student's t test. *p<0.05. ** p<0.01. *** p<0.001. ****p<0.0001. This figure was created using *BioRender.com*.

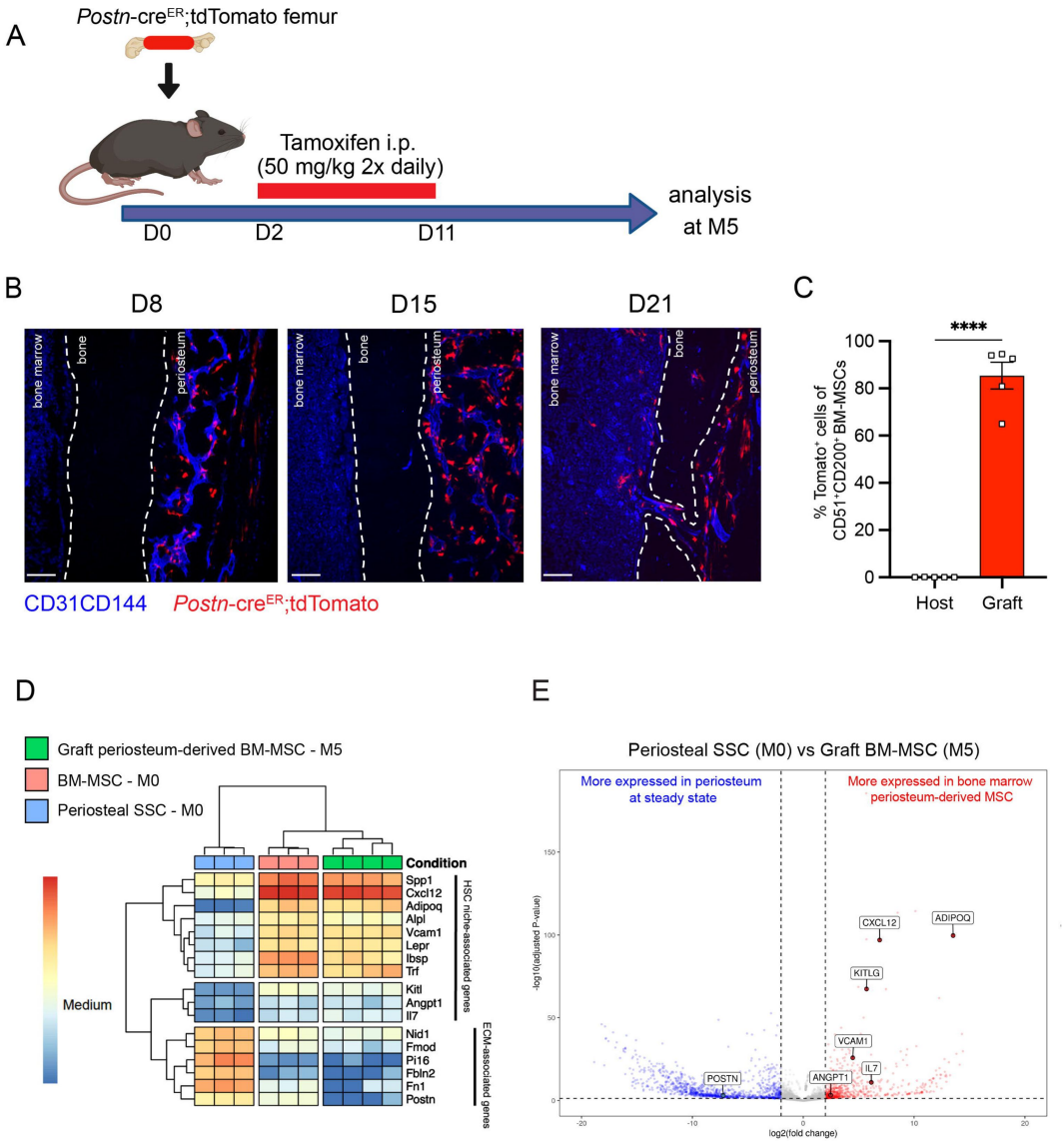

Figure 6.

Periosteum-derived graft BM-MSCs adopt characteristics of baseline BM-MSCs, including the expression of HSC niche factors.

A. Schematic illustration of the transplantation of a *Postn*-cre^{ER};tdTomato femur into a WT recipient mouse.
B. Representative whole-mount confocal z-stack projections of transplanted *Postn*-cre^{ER};tdTomato femurs into a WT recipient 8-, 15-, and 21-days after transplantation. Two-three independent experiments yielded similar results. Scale bar = 100 µm
C. Percentage of graft periosteum-derived BM-MSCs labeled Tomato^{+} five months after transplantation of a bone from a *Postn*-cre^{ER};tdTomato mouse into a WT recipient (n=5).
D. Heat map expression level of selected genes defined by previous studies for HSC niche cells and extracellular matrix genes (n=3-4).
E. Volcano plot of P-SSCs compared to graft BM-MSCs showing higher expression of HSC niche-associated genes in graft BM-MSCs.
Data are represented as the mean ± SEM. Unless otherwise noted, statistical significance was determined using unpaired two-tailed Student's t test. *p<0.05. ** p<0.01. *** p<0.001. ****p<0.0001. This figure was created using *BioRender.com*.

difference in the architecture of bone marrow vasculature was observed between the non-irradiated and irradiated limbs, no difference in P-SSCs expansion or migration into the bone marrow was detected, contrasting with the findings in our femur transplant model (Figure S7E). This observation suggests that bone transplantation results in a more severe injury to the bone marrow compared to localized irradiation, thereby enabling the assessment of BM-MSCs' recovery after more severe injury. However, it is also conceivable that stronger irradiation or a longer observation period would be necessary to observe a similar phenotype.

To examine changes in periosteum-derived BM-MSCs at the gene expression level, we performed bulk RNA sequencing on sorted $CD51^{+}CD200^{+}$Tomato+ BM-MSCs from graft *Postn*-cre^{ER};tdTomato femurs at five months after transplantation and on sorted steady-state $CD51^{+}CD200^{+}$ BM-MSCs and P-SSCs. Venn diagram and principal component analysis revealed that periosteum-derived graft BM-MSCs display a gene expression profile distinct from that of both steady state BM-MSCs and steady state P-SSCs (Figures S8A and S8B). Consistent with our previous tracing experiment using UBC-GFP periosteum (**Figure 5D**), we observed an upregulation of HSC niche-associated maintenance genes in the five-month-old graft BM-MSCs compared to P-SSCs at steady state (**Figures 6D** and **6E**). We also observed the downregulation of *Postn* and other extracellular matrix-related genes, such as fibronectin (*Fn1*) and fibromodulin (*Fmod*), in periosteum-derived graft BM-MSCs compared with P-SSCs at steady state (**Figure 6D** and **6E**). Taken together, our results indicate that P-SSCs can be reprogrammed and adapt a niche-supportive phenotype akin to native BM-MSCs after migrating into the bone marrow following acute stress and subsequent regeneration.

Discussion

Bone marrow regeneration is a critical process that enables the recovery of hematopoiesis after injury such as irradiation or chemotherapy. Bone marrow mesenchymal stromal cells represent a key component of the bone marrow microenvironment. These stromal cells play a crucial role in regulating the self-renewal, differentiation, and proliferative properties of HSCs. The periosteum, a thin membrane that is highly vascularized and innervated, is located on the outside of the bone. This membrane contains numerous skeletal stromal cells, which play a pivotal role in maintaining the bone tissue and facilitating post-fracture healing. While the bone marrow microenvironment at steady state has been extensively studied, the mechanisms of bone marrow regeneration and stromal recovery remain poorly understood. Furthermore, data related to the functions of P-SSC beyond their established role in bone maintenance and fracture healing remain scarce. The objective of this study was to develop and characterize a model of whole bone transplantation in order to study bone marrow regeneration in mice. In this model, severe injury to hematopoietic and stromal cells within the bone marrow is induced, allowing for the investigation of the regeneration process of both cell populations. We found that the total graft bone marrow cellularity and BM-MSC cellularity demonstrate a gradual increase over time, ultimately reaching levels comparable to steady state levels by five months post-transplantation. The five-month time point was subsequently employed for further analyses. Prior research has emphasized the significance of stromal integrity for the recovery of HSCs following irradiation or chemotherapy [59–61]. The findings of our study indicate that, while initially impacted by the stress associated with transplantation, BM-MSCs ultimately demonstrate their capacity to regenerate and sustain hematopoiesis within the engrafted femur. Furthermore, our findings indicate that hematopoietic progenitors derived from the graft femur are capable of engraftment in secondary recipient mice, thereby facilitating multi-lineage reconstitution. This model system recapitulates a recovering bone marrow microenvironment. Furthermore, it allows for genetic *in vivo* analysis of bone marrow regeneration. Consequently, bone transplantation can be employed as a valuable tool in future studies for investigating bone marrow regeneration.

The origin of endothelial progenitors in the bone marrow is not well defined. A recent study showed that during bone marrow regeneration after chemotherapy, sinusoidal and arteriolar vessels are derived from distinct progenitors[62]. Intriguingly, in the present study, we observed that endothelial cells within the graft originate from both the graft and host, which supports the hypothesis that different progenitors contribute to the bone marrow vascular network. Therefore, it is likely that endothelial regeneration in the graft, and vascular anastomoses between the host and graft femur are also important for the hematopoietic regeneration process. Further studies are needed to clarify the respective contributions of graft- and host-derived endothelial progenitors and the relative contributions of these different progenitor populations to regeneration of the vascular network and to hematopoietic regeneration.

Our results also highlight the high resilience and plasticity of P-SSCs and reveal their potential contribution to the bone marrow stromal network and bone marrow regeneration. At steady state, P-SSC do not express HSC maintenance genes, such as *Kitl* and *Cxcl12*, and the potential capacity of P-SSC to support HSCs has not been previously addressed. Unexpectedly, our results show that in our model, P-SSCs can migrate to the bone marrow and adopt a phenotype similar to that of BM-MSCs. Therefore, it is possible that P-SSCs can be harvested and manipulated as a source of BM-MSCs. Interestingly, we did not observe a similar migration and plasticity of P-SSCs in the context of localized femur irradiation. This observation suggests that femur transplantation introduces a greater stress on the bone marrow than irradiation, and that this increased level of stress is required to induce P-SSC plasticity and migration into the bone marrow.

In accordance with our findings, a recent study employing Gli1 to trace P-SSC demonstrated the localized expression of *Kitl* and *Cxcl12* by P-SSCs at the fracture site[43]. However, this model was not designed to specifically address the role of P-SSC in bone marrow regeneration. Furthermore, niche-specific genes were only expressed by cells adjacent to the fracture callus. Although we did not find a baseline difference in *Gli1* expression between BM-MSCs and P-SSCs in our RNA sequencing analysis, this may be due to the differences in surface markers and reporters used to identify P-SSCs and BM-MSCs. In the same study, authors did not find expression of reporters in the periosteum using the *Postn*-cre^{ER} mice. It is likely that this discrepancy is attributable to differences in generation of the Postn-Cre mice used. Indeed, previous studies have demonstrated that, compared to steady state, the *Postn* gene is upregulated following the activation of P-SSC, which is clearly evident in the context of whole bone transplantation.[63] The results of our flow cytometry and imaging analyses demonstrate that P-SSC is specifically labelled at early time points following the transplantation of grafts from Postn-Cre^{ER} mice. Therefore, we show a novel application for the use of the inducible *Postn*-cre^{ER} mice to differentiate between BM-MSCs and P-SSCs *in vivo*. Accordingly, Duchamp et al. demonstrated that periostin contributes to the highly regenerative nature of P-SSCs compared to BM-MSCs[15]. While previous studies have used *Prx1* and *Ctsk*-Cre models, these models do not adequately allow the distinction between P-SSCs and BM-MSCs, likely due to their common embryonic origin[15,16,41]. Periostin is a well-studied protein that has been shown to interact with extracellular matrix proteins and plays a key role in tissue regeneration and cancer progression, promoting proliferation, invasion, and anti-apoptotic signaling [46,64–66]. Therefore, it is possible that periostin contributes to P-SSC proliferation and migration into the bone marrow, which would be an interesting area for future investigation.

Additionally, our findings illustrate the differential stress response between BM-MSCs and P-SSCs. While BM-MSCs are renowned for their resilience to stress, our findings illustrate that P-SSCs exhibit an even greater resistance to stress, which is attributed, at least in part, to their distinctive metabolic profile[13,67]. Given that differences in apoptosis were observed between BM-MSCs and P-SSCs, even when they were cultured ex vivo under identical stress culture conditions with identical oxygen tension, it can be concluded that the observed differences between P-SSCs and BM-MSCs are due to intrinsic cellular properties rather than their anatomical location. Nevertheless, additional studies are required to elucidate the underlying mechanism responsible for the observed relative stress resistance of P-SSCs.

In conclusion, we have used a whole bone transplantation model to study bone marrow regeneration *in vivo* in response to acute injury using genetic tools. Our study has shown that through their high level of resilience and plasticity, P-SSCs can facilitate BM-MSC regeneration. Our data suggest that P-SSCs are able to contribute to hematopoietic cell recovery under stress conditions.

Experimental procedures

Mice

Mice were maintained under specific pathogen-free conditions in a barrier facility in microisolator cages. This study complied with all ethical regulations involving experiments with mice, and the Institutional Animal Care and Use Committee of Albert Einstein College of Medicine approved all experimental procedures, based on protocol #00001101. C57BL/6J mice were bred in our facilities or ordered from Jackson Laboratory. B6.129-Postn$^{tm2.1}$(cre/Esr1*)^{Jmol}/J[57] were ordered from Jackson Laboratory and then bred in our facilities. Nestin-GFP, *Gt(ROSA)26Sor*$^{tm4(ACTB-\ tdTomato,-EGFP)Luo}$*/J* (Rosa$^{mT/mG}$), C57BL/6-Tg(UBC-GFP)30Scha/J mice were bred in our facilities, Cdh5-CreER; iTdTomato mice were kindly provided by R. H. Adams (Max Planck Institute for Molecular Biomedicine, Germany) and then bred in our facilities. Unless otherwise specified, 6-to-12-week-old mice were used for the experiments. For all analytical and therapeutic experiments, sex-matched animals from the same age group were randomly assigned to experimental groups.

Bone transplantation procedure

Donor mice were anesthetized with isoflurane and euthanized by cervical dislocation. Femurs were isolated and preserved in an ice-cold phosphate-buffered saline (PBS) solution with 1% fetal bovine serum (FBS). Recipient mice were anesthetized with a ketamine/xylazine intraperitoneal injection (10 µL/g). Donor femurs were subcutaneously implanted in the back of the recipient mice, and the skin was sutured with a non-absorbable polyamide 5/0 silk. Mice were allowed to recover under a heat lamp until awake and monitored daily for up to a week post-surgery.

In vivo treatment

For lineage tracing experiments using femurs from Postn$^{tm2.1}$(cre/Esr1*)^{Jmol}/J donor mice, tamoxifen (1mg/mouse) was administered intraperitoneally to recipient mice twice daily for 10 consecutive days starting at day 2 post-transplantation.

Bone marrow transplantation

Non-competitive repopulation assays were performed using CD45.1 and CD45.2 mice. Recipient mice were lethally irradiated (12 Gy, two split doses) in a Cesium Mark 1 irradiator (JL Shepherd & Associates). A total of 1 x 10^6 CD45.2$^+$ bone marrow nuclear cells from either the graft or host femurs were obtained at five months after transplantation and injected retro-orbitally into irradiated CD45.1$^+$ mice. Mice were bled retro-orbitally every 4 weeks after bone marrow transplantation, and peripheral blood was analyzed for engraftment and repopulation up to 16 weeks.

Preparation of single cell suspensions

To isolate P-SSCs, muscle tissue was carefully removed using scissors and intact bones were submerged for 30 minutes in ice-cold PBS with 1% fetal bovine serum (FBS). The periosteum was carefully removed with a surgical blade, and mechanical dissociation was performed using scissors. Enzymatic dissociation was performed by incubating the periosteum fragments for 45 minutes at 37°C in digestion buffer (Hank's balanced salt solution (HBSS, Gibco) containing 1

mg.ml^{-1} collagenase type IV (Gibco) and 2 mg.ml^{-1} dispase (Gibco)) on a rotator. Bone marrow cells were obtained by flushing and dissociating using a 1-ml syringe with PBS via a 21-gauge needle. For analysis of stromal and endothelial cell populations, intact bone marrow plugs were flushed into digestion buffer using 21- or 25-gauge needles and incubated at 37 °C for 30 min with manual mixing every 10 mins. After bone marrow and periosteum isolation, the remaining compact bone was crushed, mechanically dissociated using scissors as previously described [45] and digested in the digestion buffer, rotating for 45 minutes at 37°C. Enzymatic digestion was stopped by adding ice-cold PEB buffer (PBS with 0.5% BSA and 2mM EDTA).

Flow cytometry and cell sorting

For FACS analysis and sorting, red blood cells were lysed (distilled H_2O containing 155mM ammonium chloride, 10mM potassium bicarbonate and 0.5M EDTA) and washed in ice-cold PEB (PBS containing 0.5% BSA and 2 mM EDTA) before staining with antibodies in PEB for 20 minutes on ice. Dead cells and debris were excluded by FSC (forward scatter), SSC (side scatter) and DAPI (4',6-diamino-2-phenylindole; Sigma). FACS analyses were carried out using BD LSRII flow cytometry (BD Biosciences) and cell sorting experiments were performed using a MoFlo Astrios (Beckman Coulter). Data were analyzed with FlowJo 10.4.0 (LCC) and FACS Diva 6.1 software (BD Biosciences). Antibodies used for FACS can be found in Supplementary table 1. For metabolic assays, cells were first stained with cell surface markers prior to labeling with metabolic dyes. For cellular ROS quantification, cells were incubated with dihydroethidium (5uM; Molecular Probes) for 20 minutes at 37°C in PBS. Glucose uptake quantification was performed by incubating the cells in DMEM without glucose (Gibco) containing Glutamax (1:100; Gibco) and 2-NBDG (17µmol mL^{-1} [1]; Cayman Chemical Company) for 30 minutes at 37°C.

CFU-F assays

For CFU-F and stromal cell culture, CD45$^-$Ter119$^-$CD31$^-$CD51$^+$CD200$^+$ stromal cells isolated from bone marrow and periosteum were sorted and plated at a clonal density (1,000 cell/well) in α-MEM (Gibco) containing 20% FBS (HyClone), 10% MesenCult Stimulatory supplement (StemCell Technologies) and 1% Penicillin-Streptomycin. Half of the medium was changed at day 7. Cells were cultured for 12-14 days, at the end of which the colonies were scored.

Osteogenic, adipogenic and chondrogenic differentiation assays

Trilineage differentiation assays towards the osteogenic, adipogenic, and chondrogenic lineages were performed as previously described[12], with minor modifications. Briefly, cells were treated with StemXVivo Osteogenic, Adipogenic, or Chondrogenic mouse differentiation media, according to the manufacturer's instructions (R&D Systems). All cultures were maintained with 5% CO2 in a water-jacketed incubator at 37°C. Osteogenic differentiation was revealed by Alizarin Red S staining. Adipocytes were identified by the typical production of lipid droplets and Bodipy (Invitrogen) staining. Chondrocytes were revealed by Alcian Blue staining.

Ex vivo culture nutrient deprivation assay

Whole bone marrow from 1 femur and whole periosteum from 2 femurs were isolated and digested as previously described and plated in α-MEM (Gibco) containing 20% FBS (HyClone), 1% penicillin-streptomycin, 1% L-glutamine and βFGF. The medium was changed every 3-4 days. Once a plate reached near confluence, CD45 lineage depletion was performed on both bone marrow and periosteum fractions. Cells were then counted and plated in 12- or 24-well plates at approximately 5000 cells/cm^2. Once the plates reached near confluence, media was switched to α-MEM without FBS, 1% L-glutamine and βFGF. 12 hours after the medium was switched to 0% FBS medium, the cells were trypsinized, spun down, and stained for cell surface markers. After 4-5 days, flow cytometric apoptosis quantification was performed using the CellEvent Caspase 3/7 kit (ThermoFisher) following the manufacturer's recommendations.

Immunofluorescence imaging of bone sections

To stain blood vessels, anti-CD31 and anti-CD144 antibodies were injected intravenously into mice (10 µg, 20 µL of 0.5 µg.µL^{-1}) and mice were sacrificed for analysis at 10 min after injection. For frozen sections of long bones, femurs and tibias were fixed in 4% paraformaldehyde (PFA) overnight at 4 °C. For cryopreservation, the bones were incubated sequentially in 10%, 20%, and 30% sucrose/PBS at 4 °C for 1h each and embedded and flash frozen in SCEM embedding medium (SECTION-LAB). Frozen sections were prepared at 20µm thickness with a cryostat (CM3050, Leica) using the Kawamoto's tape transfer method [68]. For immunofluorescence staining, sections were rinsed with PBS, post-fixed with 4% cold PFA for 10 min, followed by blocking with 20% donkey serum (DS; Sigma) in 0.5% Triton X-100/PBS for 3 h at room temperature (20–25 °C). For perilipin staining, sections were incubated for 1 hour at room temperature in saturation buffer (PBS-donkey serum 10%). The rabbit polyclonal anti-perilipin antibody (clone: D1D8; Cat: 9349; Cell Signaling Technology) was used at 1:100 dilution in 2% Donkey serum 0.1% Triton X-100/PBS overnight at 4 °C. Periostin staining was performed using whole mount femur imaging. The bone marrow was exposed by shaving the bone using a cryostat (CM3050, Leica). Shaved femurs were fixed 30 minutes at 4°C in PBS/PFA 4%. Samples were then incubated in the saturation buffer (PBS-donkey serum 10%) during 1 hour at room temperature. Polyclonal goat anti-periostin antibody (Cat: AF2955; R&D) and monoclonal rat anti-endomucin antibodies (clone: V.7C7; Cat: sc-65495; Santa Cruz) were used at a 1:100 dilution overnight at 4°C in PBS-donkey serum 2%. When necessary, primary antibody staining was followed by 3 washes with 2% DS 0.1% Triton X-100/PBS and a 30 min incubation with Alexa Fluor 568 or Alexa Fluor 488-conjugated secondary antibodies (Invitrogen) and 0.2% DAPI (4', 6-diamino-2-phenylindole; Sigma).

Image acquisition

All images were acquired at room temperature using a Zeiss Axio examiner D1 microscope (Zeiss) with a confocal scanner unit (Yokogawa) and reconstructed in three dimensions with Slide Book software (Intelligent Imaging Innovations). Image analysis was performed using both Slide Book software (Intelligent Imaging Innovations) and the Fiji build of ImageJ (NIH).

Single limb irradiation

Mice were anesthetized using isoflurane chamber and kept anesthetized throughout the procedure. Mice were irradiated using the Small Animal Radiation Research Platform, SARRP (XStrahl, Surrey, UK). Whole body lead shielding protected the mice except for one hindlimb which was protruding out from under the shield and irradiated to 20 Gy for 319 seconds in a single fraction. Mice were left under the heat lamp until they recovered.

RNA isolation and quantitative real-time PCR (q-PCR)

mRNA was purified using the Dynabeads® mRNA DIRECT™ Micro Kit (Life technologies - Invitrogen) by directly sorting stromal cells into lysis buffer, and reverse transcription was performed using RNA to cDNA EcoDry^{TM} Premix (Clontech – Takara Bio) following the manufacturer's instructions. The SYBR green (Roche) method was used for quantitative PCR using the QuantStudio 6 Flex system (Applied Biosystems, ThermoFisher). All mRNA expression levels were calculated relative to *Gapdh* or *Actb*. Supplementary table 2 lists the primer sequences used.

RNA sequencing and analysis

Total RNA from 1000-3000 sorted steady BM-MSCs, steady state P-SSCs, graft P-SSCs, and graft BM-MSCs was extracted using the RNAeasy Plus Micro kit (Qiagen) and assessed for integrity and purity using an Agilent Bioanalyzer. When applicable, RNA from two mice was combined; however, each replicate contained RNA from distinct mice. RNA-seq data generated from Illumina Novaseq6000 were processed using the following pipeline. Briefly, clean reads were mapped to the

mouse genome (GRCm38) using Spliced Transcripts Alignment to a Reference (STAR 2.6.1d). Gene expression levels were calculated and differentially expressed genes were identified using DESeq2 and enriched using clusterProfiler. All RNA sequencing data are available under the SuperSeries dataset *GSE222272* in GEO omnibus.

Statistical analysis

All data are presented as the mean±S.E.M. N represents the number of mice in each experiment, as detailed in the figure legends. No statistical method was used to predetermine sample sizes; sample sizes were determined by previous experience with similar models of hematopoiesis, as shown in previous experiments performed in our laboratory. Statistical significance was determined by an unpaired, two-tailed Student's t-test to compare two groups or a one-way ANOVA with multiple group comparisons. Statistical analyses were performed, and data presented using GraphPad Prism 8 (GraphPad Software), FACS Diva 6.1 software (BD Biosciences, FlowJo 10.4.0 (LLC), Slide Book Software 6.0 (Intelligent Imaging Innovations) and QuantStudio 6 Real-Time PCR Software (Applied Biosystem, Thermo Fisher). *P<0.05, **P<0.01, ***P<0.001, ****P<0.0001.

Data availability

RNA sequencing data from this study are available at accession number GSE222272 in the GEO Omnibus.

Acknowledgements

We would like to thank Colette Prophete and Daqian Sun for technical assistance and Lydia Tesfa and the Einstein Flow Cytometry Core Facility for expert cell sort assistance. We thank Charles Brottier and Robert Dubin of the Albert Einstein College of Medicine Computational Biology core facility for their help with analysis of RNA sequencing data. This work was supported by the National Institutes of Health (NIH) Grant 5R01DK056638 (to P.S.F. and K.G.), administrative supplement R01DK056638-23S1 (to K.E.A.), R01DK112976 (to P.S.F.), R56DK130895 (to K.G.), R01DK130895 (to K.G.), R01HL162584 (to S.P.), the NIH training Grant T32GM007288-50 (to K.E.A), and NYSTEM IIRP C029570A (to P.S.F.). T.M. was supported by the Fondation ARC pour la Recherche sur le Cancer, the Association pour le Développement de l'Hématologie Oncologie, the Société Française d'Hématologie, the Centre Hospitalier Universitaire de Rennes, and the Philip Foundation. S.T. was supported by the Japan Society for the Promotion of Science (JSPS) Postdoctoral Fellowship for Research Abroad, the Uehara Memorial Foundation Research Fellowship, and the NYSTEM Empire State Institutional Program in Stem Cell Research. M.M. was supported by the EMBO European Commission FP7 (Marie Curie Actions; EMBOCOFUND2012, GA-2012-600394, ALTF 447-2014), by the New York Stem Cell Foundation (NYSCF) Druckenmiller fellowship, and by the American Society of Hematology (ASH) Research Restart Award. S.P. was also supported by a Longevity Impetus Grant from Norn Group. This work was also supported by the Albert Einstein Cancer Center core support grant P30CA013330. Experimental figure illustrations were created using BioRender. The content is solely the responsibility of the authors and does not necessarily represent the official views of the National Institutes of Health.

Additional information

Author contributions

T.M, K.E.A, P.S.F, and K.G. designed the experiments. T.M, K.E.A, S.T., M.M. and S.P. performed the experiments and analyzed the data. T.M. and K.A. prepared the figures, and T.M., K.E.A., M.M., S.P., S.T. and K.G. wrote and edited the manuscript. P.S.F., K.G., T.L., and K.T. acquired funding for the study. J.S.V. performed the GSE222271 data analysis. A.B. conceptualized the whole bone transplantation procedure. All authors have read and approved the submitted manuscript.

Additional files

Supplementary figures.

Note

This reviewed preprint has been updated to add missing BioRender citations.

References

1 Caplan A. I. (1991) **Mesenchymal stem cells** *J Orthop Res* **9**:641–650 https://doi.org/10.1002/jor.1100090504

2 Dominici M., et al. (2006) **Minimal criteria for defining multipotent mesenchymal stromal cells. The International Society for Cellular Therapy position statement** *Cytotherapy* **8**:315–317 https://doi.org/10.1080/14653240600855905

3 Frenette P. S., Pinho S., Lucas D., Scheiermann C. (2013) **Mesenchymal stem cell: keystone of the hematopoietic stem cell niche and a stepping-stone for regenerative medicine** *Annu Rev Immunol* **31**:285–316 https://doi.org/10.1146/annurev-immunol-032712-095919

4 Kunisaki Y., et al. (2013) **Arteriolar niches maintain haematopoietic stem cell quiescence** *Nature* **502**:637–643 https://doi.org/10.1038/nature12612

5 Asada N., et al. (2017) **Differential cytokine contributions of perivascular haematopoietic stem cell niches** *Nature Cell Biology* **19**:214–223 https://doi.org/10.1038/ncb3475

6 Ding L., Saunders T. L., Enikolopov G., Morrison S. J. (2012) **Endothelial and perivascular cells maintain haematopoietic stem cells** *Nature* **481**:457–462 https://doi.org/10.1038/nature10783

7 Acar M., et al. (2015) **Deep imaging of bone marrow shows non-dividing stem cells are mainly perisinusoidal** *Nature* **526**:126–130 https://doi.org/10.1038/nature15250

8 Omatsu Y., et al. (2010) **The essential functions of adipo-osteogenic progenitors as the hematopoietic stem and progenitor cell niche** *Immunity* **33**:387–399 https://doi.org/10.1016/j.immuni.2010.08.017

9 Sugiyama T., Kohara H., Noda M., Nagasawa T. (2006) **Maintenance of the hematopoietic stem cell pool by CXCL12-CXCR4 chemokine signaling in bone marrow stromal cell niches** *Immunity* **25**:977–988 https://doi.org/10.1016/j.immuni.2006.10.016

10 Méndez-Ferrer S., et al. (2010) **Mesenchymal and haematopoietic stem cells form a unique bone marrow niche** *Nature* **466**:829–834 https://doi.org/10.1038/nature09262

11 Zhou B. O., Yue R., Murphy M. M., Peyer J. G., Morrison S. J. (2014) **Leptin-receptor-expressing mesenchymal stromal cells represent the main source of bone formed by adult bone marrow** *Cell Stem Cell* **15**:154–168 https://doi.org/10.1016/j.stem.2014.06.008

12 Pinho S., et al. (2013) **PDGFRα and CD51 mark human nestin+ sphere-forming mesenchymal stem cells capable of hematopoietic progenitor cell expansion** *J Exp Med* **210**:1351–1367 https://doi.org/10.1084/jem.20122252

13 Morikawa S., et al. (2009) **Prospective identification, isolation, and systemic transplantation of multipotent mesenchymal stem cells in murine bone marrow** *J Exp Med* **206**:2483–2496 https://doi.org/10.1084/jem.20091046

14 Chan C. K., et al. (2015) **Identification and specification of the mouse skeletal stem cell** *Cell* **160**:285–298 https://doi.org/10.1016/j.cell.2014.12.002

15 Duchamp de Lageneste O., et al. (2018) **Periosteum contains skeletal stem cells with high bone regenerative potential controlled by Periostin** *Nature Communications* **9**:773 https://doi.org/10.1038/s41467-018-03124-z

16 Debnath S., et al. (2018) **Discovery of a periosteal stem cell mediating intramembranous bone formation** *Nature* **562**:133–139 https://doi.org/10.1038/s41586-018-0554-8

17 Arnsdorf E. J., Jones L. M., Carter D. R., Jacobs C. R. (2009) **The periosteum as a cellular source for functional tissue engineering** *Tissue Eng Part A* **15**:2637–2642 https://doi.org/10.1089/ten.TEA.2008.0244

18 Ortinau L. C., et al. (2019) **Identification of Functionally Distinct Mx1+αSMA+ Periosteal Skeletal Stem Cells** *Cell Stem Cell* **25**:784–796 https://doi.org/10.1016/j.stem.2019.11.003

19 Mizoguchi T., et al. (2014) **Osterix Marks Distinct Waves of Primitive and Definitive Stromal Progenitors during Bone Marrow Development** *Developmental Cell* **29**:340–349 https://doi.org/10.1016/j.devcel.2014.03.013

20 Blashki D., Murphy M. B., Ferrari M., Simmons P. J., Tasciotti E. (2016) **Mesenchymal stem cells from cortical bone demonstrate increased clonal incidence, potency, and developmental capacity compared to their bone marrow-derived counterparts** *J Tissue Eng* **7**:2041731416661196 https://doi.org/10.1177/2041731416661196

21 Utvåg S. E., Grundnes O., Reikeraos O. (1996) **Effects of periosteal stripping on healing of segmental fractures in rats** *J Orthop Trauma* **10**:279–284 https://doi.org/10.1097/00005131-199605000-00009

22 Wang T., Zhang X., Bikle D. D. (2017) **Osteogenic Differentiation of Periosteal Cells During Fracture Healing** *J Cell Physiol* **232**:913–921 https://doi.org/10.1002/jcp.25641

23 Shapiro F. (2008) **Bone development and its relation to fracture repair. The role of mesenchymal osteoblasts and surface osteoblasts** *Eur Cell Mater* **15**:53–76 https://doi.org/10.22203/ecm.v015a05

24 Picoli C. C., et al. (2022) **Whole bone subcutaneous transplantation as a strategy to study precisely the bone marrow niche** *Stem Cell Rev Rep* https://doi.org/10.1007/s12015-022-10496-9

25 Zhou B. O., et al. (2017) **Bone marrow adipocytes promote the regeneration of stem cells and haematopoiesis by secreting SCF** *Nat Cell Biol* **19**:891–903 https://doi.org/10.1038/ncb3570

26 Yamazaki K., Allen T. D. (1991) **Ultrastructural and morphometric alterations in bone marrow stromal tissue after 7 Gy irradiation** *Blood Cells* **17**:527–549

27 Muzumdar M. D., Tasic B., Miyamichi K., Li L., Luo L. (2007) **A global double-fluorescent Cre reporter mouse** *Genesis* **45**:593–605 https://doi.org/10.1002/dvg.20335

28 Liu S., Lockhart J. R., Fontenard S., Berlett M., Ryan T. M. (2020) **Mapping the Chromosomal Insertion Site of the GFP Transgene of UBC-GFP Mice to the MHC Locus** *J Immunol* **204**:1982–1987 https://doi.org/10.4049/jimmunol.1901338

29 Wang Y., et al. (2010) **Ephrin-B2 controls VEGF-induced angiogenesis and lymphangiogenesis** *Nature* **465**:483–486 https://doi.org/10.1038/nature09002

30 Sacchetti B., et al. (2007) **Self-renewing osteoprogenitors in bone marrow sinusoids can organize a hematopoietic microenvironment** *Cell* **131**:324–336 https://doi.org/10.1016/j.cell.2007.08.025

31 Friedenstein A. J., Petrakova K. V., Kurolesova A. I., Frolova G. P. (1968) **Heterotopic of bone marrow. Analysis of precursor cells for osteogenic and hematopoietic tissues** *Transplantation* **6**:230–247

32 Tavassoli M., Crosby W. H. (1968) **Transplantation of marrow to extramedullary sites** *Science* **161**:54–56 https://doi.org/10.1126/science.161.3836.54

33 Varas F., Grande T., Ramírez A., Bueren J. A. (2000) **Implantation of bone marrow beneath the kidney capsule results in transfer not only of functional stroma but also of hematopoietic repopulating cells** *Blood* **96**:2307–2309

34 Pinho S., Frenette P. S. (2019) **Haematopoietic stem cell activity and interactions with the niche** *Nat Rev Mol Cell Biol* **20**:303–320 https://doi.org/10.1038/s41580-019-0103-9

35 Greenbaum A., et al. (2013) **CXCL12 in early mesenchymal progenitors is required for haematopoietic stem-cell maintenance** *Nature* **495**:227–230 https://doi.org/10.1038/nature11926

36 Nilsson S. K., et al. (2005) **Osteopontin, a key component of the hematopoietic stem cell niche and regulator of primitive hematopoietic progenitor cells** *Blood* **106**:1232–1239 https://doi.org/10.1182/blood-2004-11-4422

37 Stier S., et al. (2005) **Osteopontin is a hematopoietic stem cell niche component that negatively regulates stem cell pool size** *J Exp Med* **201**:1781–1791 https://doi.org/10.1084/jem.20041992

38 Arai F., et al. (2004) **Tie2/angiopoietin-1 signaling regulates hematopoietic stem cell quiescence in the bone marrow niche** *Cell* **118**:149–161 https://doi.org/10.1016/j.cell.2004.07.004

39 Jacobsen K., Kravitz J., Kincade P., Osmond D. (1996) **Adhesion receptors on bone marrow stromal cells: in vivo expression of vascular cell adhesion molecule-1 by reticular cells and sinusoidal endothelium in normal and gamma-irradiated mice** *Blood* **87**:73–82 https://doi.org/10.1182/blood.V87.1.73.73

40 Papayannopoulou T., Priestley G. V., Nakamoto B. (1998) **Anti–VLA4/VCAM-1— Induced Mobilization Requires Cooperative Signaling Through the kit/mkit Ligand Pathway** *Blood* **91**:2231–2239 https://doi.org/10.1182/blood.V91.7.2231

41 Bianco P., Gehron Robey P. (2000) **Marrow stromal stem cells** *The Journal of Clinical Investigation* **105**:1663–1668 https://doi.org/10.1172/JCI10413

42 Matsushita Y., et al. (2020) **A Wnt-mediated transformation of the bone marrow stromal cell identity orchestrates skeletal regeneration** *Nature Communications* **11**:332 https://doi.org/10.1038/s41467-019-14029-w

43 Jeffery E. C., Mann T. L. A., Pool J. A., Zhao Z., Morrison S. J. (2022) **Bone marrow and periosteal skeletal stem/progenitor cells make distinct contributions to bone maintenance and repair** *Cell Stem Cell* **29**:1547–1561 https://doi.org/10.1016/j.stem.2022.10.002

44 Mirmalek-Sani S.-H., et al. (2006) **Characterization and Multipotentiality of Human Fetal Femur–Derived Cells: Implications for Skeletal Tissue Regeneration** *Stem Cells* **24**:1042–1053 https://doi.org/10.1634/stemcells.2005-0368

45 Gulati G. S., et al. (2018) **Isolation and functional assessment of mouse skeletal stem cell lineage** *Nature Protocols* **13**:1294–1309 https://doi.org/10.1038/nprot.2018.041

46 González-González L., Alonso J. (2018) **Periostin: A Matricellular Protein With Multiple Functions in Cancer Development and Progression** *Frontiers in Oncology* **8** https://doi.org/10.3389/fonc.2018.00225

47 Horiuchi K., et al. (1999) **Identification and characterization of a novel protein, periostin, with restricted expression to periosteum and periodontal ligament and increased expression by transforming growth factor beta** *J Bone Miner Res* **14**:1239–1249 https://doi.org/10.1359/jbmr.1999.14.7.1239

48 Merle B., Garnero P. (2012) **The multiple facets of periostin in bone metabolism** *Osteoporos Int* **23**:1199–1212 https://doi.org/10.1007/s00198-011-1892-7

49 Oshima A., et al. (2002) **A novel mechanism for the regulation of osteoblast differentiation: transcription of periostin, a member of the fasciclin I family, is regulated by the bHLH transcription factor, twist** *J Cell Biochem* **86**:792–804 https://doi.org/10.1002/jcb.10272

50 Tournaire G., et al. (2020) **Nestin-GFP transgene labels skeletal progenitors in the periosteum** *Bone* **133**:115259 https://doi.org/10.1016/j.bone.2020.115259

51 Ito K., Suda T. (2014) **Metabolic requirements for the maintenance of self-renewing stem cells** *Nature Reviews Molecular Cell Biology* **15**:243–256 https://doi.org/10.1038/nrm3772

52 Suda T., Takubo K., Semenza G. L. (2011) **Metabolic regulation of hematopoietic stem cells in the hypoxic niche** *Cell Stem Cell* **9**:298–310 https://doi.org/10.1016/j.stem.2011.09.010

53 Julien A., et al. (2020) **FGFR3 in Periosteal Cells Drives Cartilage-to-Bone Transformation in Bone Repair** *Stem Cell Reports* **15**:955–967 https://doi.org/10.1016/j.stemcr.2020.08.005

54 Denhardt D. T., et al. (2003) **Transcriptional regulation of osteopontin and the metastatic phenotype: Evidence for a Ras-activated enhancer in the human OPN promoter** *Clinical & Experimental Metastasis* **20**:77–84 https://doi.org/10.1023/A:1022550721404

55 Wang W., et al. (2017) **Osteopontin activates mesenchymal stem cells to repair skin wound** *PLoS One* **12**:e0185346 https://doi.org/10.1371/journal.pone.0185346

56 Zou C., et al. (2013) **Osteopontin promotes mesenchymal stem cell migration and lessens cell stiffness via integrin β1, FAK, and ERK pathways** *Cell Biochem Biophys* **65**:455–462 https://doi.org/10.1007/s12013-012-9449-8

57 Kanisicak O., et al. (2016) **Genetic lineage tracing defines myofibroblast origin and function in the injured heart** *Nature Communications* **7**:12260 https://doi.org/10.1038/ncomms12260

58 Oka T., et al. (2007) **Genetic manipulation of periostin expression reveals a role in cardiac hypertrophy and ventricular remodeling** *Circ Res* **101**:313–321 https://doi.org/10.1161/circresaha.107.149047

59 Banfi A., Bianchi G., Galotto M., Cancedda R., Quarto R. (2001) **Bone Marrow Stromal Damage after Chemo/Radiotherapy: Occurrence, Consequences and Possibilities of Treatment** *Leukemia & Lymphoma* **42**:863–870 https://doi.org/10.3109/10428190109097705

60 Lucas D., et al. (2013) **Chemotherapy-induced bone marrow nerve injury impairs hematopoietic regeneration** *Nature Medicine* **19**:695–703 https://doi.org/10.1038/nm.3155

61 Hérodin F., Drouet M. (2005) **Cytokine-based treatment of accidentally irradiated victims and new approaches** *Exp Hematol* **33**:1071–1080 https://doi.org/10.1016/j.exphem.2005.04.007

62 Xu C., et al. (2018) **Stem cell factor is selectively secreted by arterial endothelial cells in bone marrow** *Nature Communications* **9**:2449 https://doi.org/10.1038/s41467-018-04726-3

63 Duchamp de Lageneste O., et al. (2018) **Periosteum contains skeletal stem cells with high bone regenerative potential controlled by Periostin** *Nat Commun* **9**:773 https://doi.org/10.1038/s41467-018-03124-z

64 Bao S., et al. (2004) **Periostin potently promotes metastatic growth of colon cancer by augmenting cell survival via the Akt/PKB pathway** *Cancer Cell* **5**:329–339 https://doi.org/10.1016/S1535-6108(04)00081-9

65 Butcher J. T., Norris R. A., Hoffman S., Mjaatvedt C. H., Markwald R. R. (2007) **Periostin promotes atrioventricular mesenchyme matrix invasion and remodeling mediated by integrin signaling through Rho/PI 3-kinase** *Developmental Biology* **302**:256–266 https://doi.org/10.1016/j.ydbio.2006.09.048

66 Conway S. J., et al. (2014) **The role of periostin in tissue remodeling across health and disease** *Cellular and Molecular Life Sciences* **71**:1279–1288 https://doi.org/10.1007/s00018-013-1494-y

67 Haas R. J., Bohne F., Fliedner T. M. (1969) **On the Development of Slowly-turning-over Cell Types in Neonatal Rat Bone Marrow (Studies Utilizing the Complete Tritiated Thymidine Labeling Method Complemented by C-14 Thymidine Administration)** *Blood* **34**:791–805 https://doi.org/10.1182/blood.V34.6.791.791

68 Kawamoto T., Shimizu M. (2000) **A method for preparing 2-to 50-micron-thick fresh-frozen sections of large samples and undecalcified hard tissues** *Histochem Cell Biol* **113**:331–339 https://doi.org/10.1007/s004180000149

Author information

Tony Marchand[#]

Service d'hématologie Clinique, Centre Hospitalier Universitaire de Rennes, Rennes, France, UMR U1236, INSERM, Université Rennes, EFS Bretagne, Equipe Labellisée Ligue Contre le Cancer, Rennes, France, Ruth L. and David S. Gottesman Institute for Stem Cell and

Regenerative Medicine, Albert Einstein College of Medicine, Michael F. Price Center, Bronx, United States, Department of Cell Biology, Albert Einstein College of Medicine, Michael F. Price Center, Bronx, United States

For correspondence: tony.marchand@chu-rennes.fr

[#]These authors contributed equally to this work.

Kemi E Akinnola[#]

Ruth L. and David S. Gottesman Institute for Stem Cell and Regenerative Medicine, Albert Einstein College of Medicine, Michael F. Price Center, Bronx, United States, Department of Cell Biology, Albert Einstein College of Medicine, Michael F. Price Center, Bronx, United States

[#]These authors contributed equally to this work.

Shoichiro Takeishi

Ruth L. and David S. Gottesman Institute for Stem Cell and Regenerative Medicine, Albert Einstein College of Medicine, Michael F. Price Center, Bronx, United States, Department of Cell Biology, Albert Einstein College of Medicine, Michael F. Price Center, Bronx, United States

Maria Maryanovich

Ruth L. and David S. Gottesman Institute for Stem Cell and Regenerative Medicine, Albert Einstein College of Medicine, Michael F. Price Center, Bronx, United States, Department of Cell Biology, Albert Einstein College of Medicine, Michael F. Price Center, Bronx, United States

Sandra Pinho

Ruth L. and David S. Gottesman Institute for Stem Cell and Regenerative Medicine, Albert Einstein College of Medicine, Michael F. Price Center, Bronx, United States, Department of Cell Biology, Albert Einstein College of Medicine, Michael F. Price Center, Bronx, United States, Department of Medical Oncology, Albert Einstein College of Medicine, Bronx, United States, Department of Pharmacology & Regenerative Medicine, University of Illinois at Chicago, Chicago, United States

Julien Saint-Vanne

UMR U1236, INSERM, Université Rennes, EFS Bretagne, Equipe Labellisée Ligue Contre le Cancer, Rennes, France

Alexander Birbrair

Ruth L. and David S. Gottesman Institute for Stem Cell and Regenerative Medicine, Albert Einstein College of Medicine, Michael F. Price Center, Bronx, United States, Department of Cell Biology, Albert Einstein College of Medicine, Michael F. Price Center, Bronx, United States, Department of Dermatology, University of Wisconsin-Madison, Madison, United States

Thierry Lamy

Service d'hématologie Clinique, Centre Hospitalier Universitaire de Rennes, Rennes, France, UMR U1236, INSERM, Université Rennes, EFS Bretagne, Equipe Labellisée Ligue Contre le Cancer, Rennes, France

Karin Tarte

UMR U1236, INSERM, Université Rennes, EFS Bretagne, Equipe Labellisée Ligue Contre le Cancer, Rennes, France, Laboratoire Suivi Immunologique des Thérapeutiques Innovantes, Centre Hospitalier Universitaire de Rennes, Rennes, France

ORCID iD: 0000-0002-6809-917X

Paul S Frenette[†]
Ruth L. and David S. Gottesman Institute for Stem Cell and Regenerative Medicine, Albert Einstein College of Medicine, Michael F. Price Center, Bronx, United States, Department of Cell Biology, Albert Einstein College of Medicine, Michael F. Price Center, Bronx, United States, Department of Medical Oncology, Albert Einstein College of Medicine, Bronx, United States

[†]Deceased

Kira Gritsman
Ruth L. and David S. Gottesman Institute for Stem Cell and Regenerative Medicine, Albert Einstein College of Medicine, Michael F. Price Center, Bronx, United States, Department of Cell Biology, Albert Einstein College of Medicine, Michael F. Price Center, Bronx, United States, Department of Medical Oncology, Albert Einstein College of Medicine, Bronx, United States
ORCID iD: 0000-0002-1367-1167

For correspondence: kira.gritsman@einsteinmed.edu

Editors

Reviewing Editor
Rio Sugimura
The University of Hong Kong, Pok Fu Lam, Hong Kong

Senior Editor
Kathryn Cheah
University of Hong Kong, Hong Kong, Hong Kong

Reviewer #1 (Public review):

Summary:

The manuscript under review investigates the role of periosteal stem cells (P-SSC) in bone marrow regeneration using a whole bone subcutaneous transplantation model. While the model is somewhat artificial, the findings were interesting, suggesting the migration of periosteal stem cells into the bone marrow and their potential to become bone marrow stromal cells. This indicates a significant plasticity of P-SSC consistent with previous reports using fracture models (Cell Stem Cell 29:1547, Dev Cell 59:1192).

Major comments from previous round of review:

(1) The authors assert that the periosteal layer was completely removed in their model, which is crucial for their conclusions. To substantiate this claim, it is recommended that the authors provide evidence of the successful removal of the entire periosteal stem cell (P-SSC) population. A colony-forming assay, with and without periosteal removal, could serve as a suitable method to demonstrate this.

(2) The observation that P-SSCs do not express Kitl or Cxcl12, while their bone marrow stromal cell (BM-MSC) derivatives do, is a key finding. To strengthen this conclusion, the authors are encouraged to repeat the experiment using Cxcl12 or Scf reporter alleles. Immunofluorescence staining that confirms the migration of periosteal cells and their transformation into Cxcl12- or Scf-reporter-positive cells would significantly enhance the paper's key conclusion.

(3) On page 8, line 20, the authors' statement regarding the detection of Periostin+ cells outside the periosteum layer could be misinterpreted due to the use of the periostin antibody. Given that periostin is an extracellular matrix protein, the staining may not accurately represent Periostin-expressing cells but rather the presence of periostin in the extracellular matrix. The authors should revise this section for greater precision.

Comments on revised version:

My comments from the previous round of review have mostly been addressed.

https://doi.org/10.7554/eLife.101714.2.sa2

Reviewer #2 (Public review):

Summary:

The authors have established a femur graft model that allows the study of hematopoietic regeneration following transplantation. They have extensively characterized this model, demonstrating the loss of hematopoietic cells from the donor femur following transplantation, with recovery of hematopoiesis from recipient cells. They also show evidence that BM MSCs present in the graft following transplantation are graft-derived. They have utilized this model to show that following transplantation, periosteal cells respond by first expanding, then giving rise to more periosteal SSCs, then migrating into the marrow to give rise to BM MSCs.

Strengths:

These studies are notable in several ways: 1) establishment of a novel femur graft model for the study of hematopoiesis; 2) Use of lineage tracing and surgery models to demonstrate that periosteal cells can give rise to BM MSCs.

Weaknesses:

There are a few weaknesses. First, the authors do not definitively demonstrate the requirement of periosteal SSC movement into the BM cavity for hematopoietic recovery. Hematopoiesis recovers significantly before 5 months, even before significant P-SSC movement has been shown, and hematopoiesis recovers significantly even when periosteum has been stripped. Second, it is not clear how the periosteum is changing in the grafts. Which cells are expanding is unclear, and it is not clear if these cells have already adopted a more MSC-like phenotype prior to entering the marrow space. Indeed, given the presence of host-derived endothelial cells in the BM, these studies are reminiscent of prior studies from this group and others that re-endothelialization of the marrow may be much more important for determining hematopoietic regeneration, rather the P-SSC migration. Third, the studies exploring the preferential depletion of BM MSCs vs P-SSCs are difficult to interpret. The single metabolic stress condition chosen was not well-justified, and the use of purified cell populations to study response to stress ex vivo may have introduced artifacts into the system.

Comments on the current version: The authors have addressed my concerns adequately

https://doi.org/10.7554/eLife.101714.2.sa1

Author response:

The following is the authors' response to the original reviews.

> ***Public Reviews:***
>
> ***Reviewer #1 (Public review):***
>
> *The manuscript under review investigates the role of periosteal stem cells (P-SSC) in bone marrow regeneration using a whole-bone subcutaneous transplantation model. While the model is somewhat artificial, the findings were interesting, suggesting the migration of periosteal stem cells into the bone marrow and their potential to become bone marrow stromal cells. This indicates a significant plasticity of P-SSC consistent with previous reports using fracture models (Cell Stem Cell 29:1547, Dev Cell 59:1192).*
>
> *Major Concerns*
>
> *(1) The authors assert that the periosteal layer was completely removed in their model, which is crucial for their conclusions. To substantiate this claim, it is recommended that the authors provide evidence of the successful removal of the entire periosteal stem cell (P-SSC) population. A colony-forming assay, with and without periosteal removal, could serve as a suitable method to demonstrate this.*

We are grateful to the reviewer for this valuable suggestion. The objective of this experiment was to demonstrate that periosteal ablation impairs bone marrow regeneration, a finding that is supported by our results. We expect that ablation of the periosteum would be associated with only a partial decrease in CFU-F activity, given the presence of MSCs in the bone and in the endosteal region of the bone marrow. Therefore, CFU-F assays would be difficult to interpret in this setting. In view of the phenotype obtained, providing proof of concept of the importance of the periosteum, we do not believe that further experiments would strengthen the level of proof of this experiment.

> *(2) The observation that P-SSCs do not express Kitl or Cxcl12, while their bone marrow stromal cell (BM-MSC) derivatives do, is a key finding. To strengthen this conclusion, the authors are encouraged to repeat the experiment using Cxcl12 or Scf reporter alleles. Immunofluorescence staining that confirms the migration of periosteal cells and their transformation into Cxcl12- or Scf-reporter-positive cells would significantly enhance the paper's key conclusion.*

Transplantation of periosteum isolated from Cxcl12 or Scf into WT bones is an excellent suggestion. Indeed, this experiment would confirm (1) the migration of periosteal SSC and (2) the expression of Cxcl12 and Scf by BM-MSCs derived from the periosteum .However, it should be noted that the current limitations in terms of available resources preclude the execution of these experiments. Moreover, the use of the PostnCre^{ER};Tmt mice represent the optimal approach for tracking and specifically isolating BM-MSCs derived from the periosteum. The expression of Cxcl12 and Scf by BM-MSCs derived from the periosteum has been demonstrated in 2 distinct experimental models (Figures 5 and 6).

> *(3) On page 8, line 20, the authors' statement regarding the detection of Periostin+ cells outside the periosteum layer could be misinterpreted due to the use of the periostin antibody. Given that periostin is an extracellular matrix protein, the staining may not accurately represent Periostin-expressing cells but rather the presence of periostin in the extracellular matrix. The authors should revise this section for greater precision.*

We acknowledge and appreciate the reviewer's attention to detail. This is, in fact, an error. Nestin-GFP positive periosteal SSC are seen within the periosteum marked by an anti-periostin antibody labeling the extracellular matrix of the periosteum. The manuscript has been revised to address this inaccuracy on page 9, lines 8-9.

> ***Reviewer #2 (Public review):***
>
> *Summary:*
>
> *The authors have established a femur graft model that allows the study of hematopoietic regeneration following transplantation. They have extensively characterized this model, demonstrating the loss of hematopoietic cells from the donor femur following transplantation, with recovery of hematopoiesis from recipient cells. They also show evidence that BM MSCs present in the graft following transplantation are graft-derived. They have utilized this model to show that following transplantation, periosteal cells respond by first expanding, then giving rise to more periosteal SSCs, and then migrating into the marrow to give rise to BM MSCs.*
>
> *Strengths:*
>
> *These studies are notable in several ways:*
>
> *(1) Establishment of a novel femur graft model for the study of hematopoiesis;*
>
> *(2) Use of lineage tracing and surgery models to demonstrate that periosteal cells can give rise to BM MSCs.*

We thank the reviewer for noting the novelty of our manuscript.

> *Weaknesses:*
>
> *There are a few weaknesses. First, the authors do not definitively demonstrate the requirement of periosteal SSC movement into the BM cavity for hematopoietic recovery. Hematopoiesis recovers significantly before 5 months, even before significant P-SSC movement has been shown, and hematopoiesis recovers significantly even when periosteum has been stripped.*
>
> *This is an important point. Notably, we can see expansion of P-SSCs by day 8 after femur transplantation and evidence of periosteum-derived SSCs in the bone marrow by day 15, before we can detect any significant hematopoietic recovery (see Figure 3A-C).*
>
> *Second, it is not clear how the periosteum is changing in the grafts. Which cells are expanding is unclear, and it is not clear if these cells have already adopted a more MSC-like phenotype prior to entering the marrow space.*
>
> *This is an interesting question. To examine early changes in gene expression in periosteal SSCs in grafted femurs, we performed additional RNA sequencing on host periosteal SSCs vs periosteal SSCs from grafted femurs at an earlier time point - at 3 days after femur transplantation and on host bone marrow MSCs (see new Supplementary Figure S5 A-C). At this time point the three cell populations are already distinct on the PCA plot (Figure S5A), and there is downregulation of some periosteal genes in the graft P-SSCs (Figure S5B). However, we do not yet see upregulation of Kitl or Cxcl12 or most other BM MSC genes in graft P-SSCs at this time point (Figure S5B). Furthermore, gene set enrichment analysis (GSEA) revealed upregulation of cell cycle, DNA replication and mismatch repair gene signatures, and downregulation of multiple gene signatures compared to host P-SSCs (Figure S5C). Therefore, we conclude that P-SSCs already adopt some gene expression changes early after femur transplantation, but have not yet fully differentiated into BM MSCs at this early time point. This experiment is now discussed on p.10 of the revised manuscript.*

> *Indeed, given the presence of host-derived endothelial cells in the BM, these studies are reminiscent of prior studies from this group and others that re-endothelialization of the marrow may be much more important for determining hematopoietic regeneration, rather than the P-SSC migration.*

Indeed, as previously shown by our group and others, we agree that endothelial regeneration and re-endothelialization may also play an important role in this bone marrow regeneration model. It is noteworthy that this model has the potential to serve as a valuable tool for analyzing the origin of BM endothelial cells during regeneration processes. To further illustrate the endothelial regeneration, additional images of bone sections from VE-cadherin-cre;TdTomato grafted femurs at 15 days, one month, and five months post-transplantation have been included in the new Figure S3. These images reveal extensive vascularization of the graft and proximity of UBC-GFP+ donor-derived vessels to VE-cadherin+ host-derived blood vessels in the bone marrow within one month (see Figure S2C). This observation is consistent with the timing of both BM MSC recovery and HSC recovery in the grafts, thereby suggesting the importance of endothelial recovery (see Fig. 1B). A new discussion of these findings has been included on page 6 of the revised manuscript and on page 16 in the discussion section.

> *Third, the studies exploring the preferential depletion of BM MSCs vs P-SSCs are difficult to interpret. The single metabolic stress condition chosen was not well-justified, and the use of purified cell populations to study response to stress ex vivo may have introduced artifacts into the system.*

We chose to focus on hypoxia as the main condition in which to analyze the stress response of P-SSCs vs BM MSCs because we reasoned that due to the location of P-SSCs on the outside of the bone, these cells would be exposed to a higher oxygen tension than BM-MSCs, which are located within the bone marrow. Therefore, we wanted to determine whether this exposure to a different oxygen tension would be sufficient to explain the different properties of P-SSCs and BM MSCs. We modified the text on p.11 of the manuscript to explain the rationale for this experiment better.

> ***Reviewer #3 (Public review):***
>
> *Summary:*
>
> *Marchand, Akinnola, et al. describe the use of the novel model to study BM regeneration. Here, they harvest intact femurs and subcutaneously graft them into recipient mice. Similar to standard BM regeneration models, there is a rapid decrease in cellularity followed by a gradual recovery over 5 months within the grafts. At 5 months, these grafts have robust HSC activity, similar to HSCs isolated from the host femur. They find that periosteum skeletal stem cells (p-SSCs) are the primary source of BM-MSCs within the grafted femur and that these cells are more resistant to the acute stress of grafting the femur.*
>
> *Strengths:*
>
> *This is an interesting manuscript that describes a novel model to study BM regeneration. The model has tremendous promise.*

We thank the reviewer for highlighting the novelty and potential of our work.

> *Weaknesses:*

The authors claim that grafting intact femurs subcutaneously is a model of BM regeneration and can be used as a replacement for gold standard BM regeneration assays such as sublethal chemo/irradiation. However, there isn't enough explanation as to how this model is equivalent or superior to the traditional models. For instance, the authors claim that this model allows for the study of "BM regeneration in vivo in response to acute injury using genetic tools." This can and has been done numerous times with established, physiologically relevant BM regeneration models. The onus is on the authors to discuss or perform the necessary experiments to justify the use of this model. For example, standard BM regeneration models involve systemic damage that is akin to therapies that require BM regeneration. How is studying the current model that provides only an acute injury more relevant and useful than other models? As it stands, it seems as if the authors could have done all the experiments demonstrating the importance of these p-SSCs in the traditional myelosuppressive BM regeneration models to be more physiologically relevant. Along these lines, the use of a standard BM regeneration model (e.g., sublethal chemo/irradiation) as a critical control is missing and should be included. Even if the control doesn't demonstrate that p-SSCs can contribute to the BM-MSC during regeneration, it will still be important because it could be the justification for using the described model to specifically study p-SSCs' regulation of BM regeneration.

We appreciate the reviewer raising this important point. We never intended this femur transplantation model of bone marrow injury to replace more established models, such as chemotherapy or irradiation. In fact, we compared the effects of femur transplantation to localized bone irradiation on P-SSCs using our Periostin-Cre;Td-Tomato lineage tracing model. We found that irradiation does not induce the same migration of Tomato+ P-SSCs from the periosteum to the bone marrow cavity the way that femur transplantation, and cannot be used to demonstrate the plasticity of P-SSCs in the same way (see new Supplementary Figure S7D-E). Therefore, this appears to be a more severe form of bone marrow injury, and is not similar to other more established assays of bone marrow injury. We also added this discussion to the revised manuscript on p.14 and in the discussion section on p.17.

The authors perform some analysis that suggests that grafting a whole femur mimics BM regeneration, but there are many experiments missing from the manuscript that will be necessary to support the use of this model. To demonstrate that this new model mimics current BM regeneration models, the authors need to perform a careful examination of the early kinetics of hematopoietic recovery post-transplant. Complete blood counts should be performed on the grafts, focusing on white blood cells (particularly neutrophils), red blood cells, platelets, all critical indicators of BM regeneration. This analysis should be done at early time points that include weekly analysis for a minimum of 28 days following the graft. Additionally, understanding how and when the vasculature recovers is critical. This is particularly important because it is well-established that if there is a delay in vascular recovery, there is a delay in hematopoietic recovery. As mentioned above, a standard BM regeneration model should be used as a control.

We concur with the reviewer that hematopoietic recovery is a pivotal aspect of this model. We conducted a time-course analysis of bone marrow and HSC cellularity from day 0 to month 5 post-transplantation (Figure 1B). Furthermore, we evaluated the HSC capacities through bone marrow transplantation from grafted or host femurs (Figures 1D and 1E) and quantified the various hematopoietic cells in the graft after five months (Supplemental Figure 1). Furthermore, hematopoiesis occurring in the transplanted bone was comprehensively evaluated in another article, currently in revision and available in BioRxiv (Takeishi, S., Marchand, T., Koba, W. R., Borger, D. K., Xu, C., Guha, C., Bergman, A., Frenette, P. S., Gritsman,

K., & Steidl, U. (2023). Haematopoietic stem cell numbers are not solely determined by niche availability. bioRxiv: the preprint server for biology, 2023.10.28.564559. https://doi.org/10.1101/2023.10.28.564559). We did not use another assay of bone marrow regeneration as a "control", since we do not expect to see similar plasticity of periosteal SSCs in these models, such as with the localized irradiation model described in the new Figure S7D-E.

We agree with the reviewer that endothelial recovery is also likely to be very important for hematopoietic recovery in this model, but this was not the focus of this manuscript. The process of endothelial recovery is likely to be more complex than that of MSC recovery, as our findings indicate that the graft endothelium can arise from both the host and the graft femur (see Fig.2D). Consequently, further investigation into the mechanisms of endothelial recovery and its contribution to hematopoiesis in this experimental system will be an interesting focus of future work. We believe that this bone transplantation model represents a valuable tool for addressing questions regarding the origin and regeneration mechanisms of bone marrow endothelial cells.

> *The contribution of donor and host cells to the BM regeneration of the graft is interesting. Particularly, the chimerism of the vasculature. One can assume that for the graft to undergo BM regeneration, there needs to be the delivery of nutrients into the graft via the vasculature. The chimerism of the vascular network suggests that host endothelial cells anastomose with the graft. Host mice should have their vascular system labeled with a dye such as dextran to determine if anastomosis has occurred. If not, the authors need to explain how this graft survives up to 5 months. If anastomosis does occur, then it is very surprising that the hematopoietic system of the graft is not a chimera because this would essentially be a parabiosis model. This needs to be explained.*

We have included additional images of bone sections from VE-cadherin-cre;tdTomato grafted femurs at 15 days, one month, and five months post transplantation in the new Figure S3. These images show extensive vascularization of the graft and proximity of UBC-GFP+ donor-derived vessels to VE-cadherin+ host-derived blood vessels in the bone marrow within one month, suggesting a potential anastomosis (Figure S2C). However, it is not surprising that hematopoiesis arises exclusively from the host, as we observed complete death of the hematopoietic cells and BM MSCs in the graft femur within the first 3 days of femur transplantation (see Figure S1A), and we do not see any significant hematopoietic recovery in the grafts until at least 2 months (see Fig.1B). Therefore, this is not similar to a parabiosis model, as confirmed by our chimerism studies shown in Figure 2D. In addition, these data are consistent with the results reported with the use of ossicles (doi:10.1038/nature09262; DOI 10.1016/j.cell.2007.08.025; doi:10.1038/nature07547).

> *Most of the data presented for the resistance of p-SSCs to stress suggests DNA damage response. Do p-SSCs demonstrate a higher ability to resolve DNA damage? Do they accumulate less DNA damage? Staining for DNA damage foci or performing comet assays could be done to further define the mechanism of stress resistance properties of p-SSCs.*

This is an interesting question. In our RNA sequencing analysis of graft P-SSCs compared with host P-SSCs we did observe an upregulation of mismatch repair gene signatures by gene set enrichment analysis (GSEA) (new Figure S5C). Therefore, it is possible that P-SSCs do have an altered DNA damage response. However, we are unable to investigate this further at this time.

> *Given the importance of BM-MSCs in hematopoiesis and that the majority of the emerging BM-MSCs appear to be derived from p-SSCs, the authors should perform*

> *experiments to determine if p-SSC-derived BM-MSCs are critical regulators of BM regeneration. For example, the authors could test this by crossing the Postn-creER mice with iDTR mice to ablate these cells and see if recovery is inhibited or delayed. This should be done with the described periosteum-wrapped femur graft model as well as a control BM regeneration model. Demonstrating that the deletion of these cells affects BM regeneration in both models would further justify the physiological relevance and utility of the femur graft model.*

We thank the reviewer for this excellent suggestion, and we agree that this is an important experiment. However, our attempts to ablate Postn+ cells using the iDTA system were limited by technical difficulties, which we are unable to address at this time.

> ***Recommendations for the authors:***
>
> ***Reviewer #1 (Recommendations for the authors):***
>
> *(1) In Figure 2C, the vascular network staining appears to be duplicated, suggesting a possible error in image capture. The authors should replace this image with a different field or an alternative picture to avoid confusion.*

We thank the reviewer for noting this accidental duplication due to an image stitching problem. Figure 2C was replaced by a different image from the same experiment.

> *(2) For consistency and clarity, a scale bar should be included in Figure S3E to indicate that the magnification factors of the respective visual fields are identical.*

We thank the reviewer for highlighting this point. The magnification used has been added in the revised Figure.

> *(3) In Figure S5B, the difference in normalized Opn mRNA expression relative to Gapdh between steady-state BM-MSCs and P-SSCs seems substantial, which contradicts the "ns" (not significant) label. The authors should verify the accuracy of this labeling.*

We agree with the reviewer that this difference in what is now Figure S6B looks substantial. However, we confirmed that this difference is not statistically significant, likely due to the high variability between replicates in Opn expression in the steady state BM MSCs.

> ***Reviewer #2 (Recommendations for the authors):***
>
> *In order to strengthen the argument that P-SSCs are necessary for hematopoietic recovery, the authors should consider providing the following data:*
>
> *(1) In the periosteal stripping experiments, the authors should show if periosteum-derived MSCs are present in the BM throughout the process of hematopoietic recovery (not just at the end of the experiment). If none are present at the end, that would mean that periosteum is not required for hematopoietic recovery, but would still suggest that it is required for optimal hematopoietic recovery. At early time points, it would also be very helpful to demonstrate the composition and amount of endothelium present in the marrow to determine if P-SSC migration and differentiation into MSCs depends on endothelial reconstitution.*

To further examine the vascularization of the transplanted femur at an earlier time point, we have added additional images of grafted femur from VE-cadherin-cre;tdTomato at 15 days and one month post transplantation in the new Figure S3A and S3B. These images already show extensive vascularization of the graft periosteum stained with an anti-periostin

antibody. In addition, we observed anastomoses of host VE-cadherin;Tmt+ blood vessels with graft ubc-GFP+ blood vessels in the grafted periosteum within one month (Figure S3C).

> *(2) Studies of the surgical periosteum grafts could benefit from histologic analysis of the BM and its MSC components at earlier time points following grafting since the data provided are only at 5 months. Such studies would allow a better appreciation of the relationship between P-SSC migration into the marrow and hematopoietic recovery.*

We have performed histologic analysis of grafted femurs at multiple early time points, which shows expansion of P-SSCs and their migration into the bone marrow cavity (Figure 3C).

> *(3) Studies of stress responses preferably should be performed using intact bone and should characterize P-SSC and BM MSC apoptosis, cell cycle status, differentiation, etc, immediately following shifts to the stress conditions. These studies would be more compelling if performed using additional "stress" conditions likely to represent the graft environment.*

This is an interesting suggestion. However, these types of studies would not be possible in intact bones ex vivo, as P-SSCs are known to migrate out of the bone in culture.

https://doi.org/10.7554/eLife.101714.2.sa0